THESIS FOR THE DEGREE OF DOCTOR OF PHILOSOPHY

Three-Dimensional Modelling of Bond in Reinforced Concrete

Theoretical Model, Experiments and Applications

KARIN LUNDGREN

Division of Concrete Structures

Department of Structural Engineering

Chalmers University of Technology

Göteborg, Sweden 1999

Three-Dimensional Modelling of Bond in Reinforced Concrete
Theoretical Model, Experiments and Applications
KARIN LUNDGREN
ISBN 91-7197-853-4

Cover:
Results from analyses of a frame corner with a short splice are visualised. The red colour indicates cracked concrete; shown enlarged is the splitting crack that is a result of the bond action at the splice. For more information, see Paper IV, page 14.

Three-Dimensional Modelling of Bond in Reinforced Concrete

Theoretical Model, Experiments and Applications

KARIN LUNDGREN

Division of Concrete Structures

Department of Structural Engineering

Chalmers University of Technology

ABSTRACT

The bond mechanism between deformed bars and concrete is known to be influenced by multiple parameters, such as the strength of the surrounding structure, the occurrence of splitting cracks in the concrete and the yielding of the reinforcement. However, when reinforced concrete structures are analysed using the finite element method, it is quite common to assume that the bond stress depends solely on the slip. A new theoretical model which is especially suited for detailed three-dimensional analyses was developed. In the new model, the splitting stresses of the bond action are included; furthermore, the bond stress depends not only on the slip, but also on the radial deformation between the reinforcement bar and the concrete. In addition, this model includes the simulation of cyclic loading. Steel-encased pull-out tests subjected to reversed cyclic loading were carried out. The tangential strain in the steel tubes was measured to investigate how the splitting stresses are affected by cyclic loading. Based on the results of these tests, several improvements of the model were made. Bar pull-out tests with differing geometries and with both monotonic and cyclic loading were analysed, using the new model for the bond action, and non-linear fracture mechanics for the concrete. The results show that the model is capable of dealing with a variety of failure modes, such as pull-out failure, splitting failure, and the loss of bond when the reinforcement is yielding, as well as dealing with cyclic loading in a physically reasonable way.

The new model was used in detailed three-dimensional analyses of frame corners. Until recently, splicing of the reinforcement in frame corners had not been allowed by the Swedish Road Administration. Since this had led to reinforcement detailing that was hard to realise on site, it was of interest to examine how splicing of the reinforcement affects the behaviour of the structure. Tests on frame corners subjected to closing moments were also carried out. It was found that the analyses could describe the test performance in a reasonable way. The tests and analyses showed that splicing the reinforcement in the middle of the corner has advantages over splices placed outside the bend of the reinforcement. They also indicated, in agreement with previous work, that provided the splice length is as long as required in the codes, there are no disadvantages in splicing the reinforcement within the corner of a frame subjected to closing moment.

Key words: Reinforced concrete, bond, splitting effects, three-dimensional analysis, pull-out tests, cyclic loading, finite element analysis, non-linear fracture mechanics, splicing of reinforcement, frame corners.

I

Tredimensionell modellering av vidhäftning i armerad betong
Teoretisk modell, experiment och tillämpningar
KARIN LUNDGREN
Avdelningen för betongbyggnad
Instutionen för konstruktionsteknik
Chalmers tekniska högskola

SAMMANFATTNING

Vidhäftningsmekanismen mellan kamstänger och betong påverkas av ett antal parametrar, såsom hållfastheten hos den omgivande strukturen, uppkomsten av spjälksprickor i betongen och om armeringen flyter. När armerade betong-konstruktioner analyseras med finita elementmetoden antas dock vanligtvis att vidhäftningen beror enbart på glidningen. En ny teoretisk modell har utvecklats, som är speciellt lämpad för detaljerade tredimensionella analyser. I denna nya modell är spjälkspänningarna som uppstår på grund av vidhäftningen inkluderade, och vidhäftningen beror inte enbart på glidningen, utan också på den radiella deformationen mellan armeringsjärnet och betongen. Modellen har även utvecklats för simulering av cyklisk last. Stålmantlade utdragsförsök med cyklisk belastning har utförts. De tangentiella töjningarna i stålrören mättes för att undersöka hur den cykliska lasten påverkar spjälkspänningarna. Utgående från resultaten i dessa försök gjordes flera förbättringar i modellen. Den nya modellen som beskriver vidhäftningsmekanismen har använts, tillsammans med icke-linjär brottmekanik för att beskriva betongen, i analyser av utdragsförsök med olika geometrier och med både monoton och cyklisk belastning. Resultaten visar att den nya modellen kan hantera olika brottyper, som utdragsbrott, spjälkbrott, att vidhäftningen minskar när armeringen flyter, samt att den kan simulera cyklisk last på ett fysikaliskt rimligt sätt.

Den nya vidhäftningsmodellen har använts i detaljerade tredimensionella analyser av ramhörn. Tidigare har Vägverket inte tillåtit att armeringen skarvas inom ramhörnet. Eftersom det ledde till komplicerade detaljutformningar som var svåra att utföra, var det av intresse att undersöka hur armeringsskarvar inom hörnområdet påverkar det strukturella uppförandet. Ramhörn har provats med stängande moment. Det visade sig att analyserna kunde beskriva försöksresultaten på ett rimligt sätt. Försöken och analyserna visade att det är fördelaktigt att skarva armeringen mitt i hörnet, jämfört med att placera skarven utanför armeringsbocken. De indikerar också, liksom tidigare analyser och försök, att om skarvlängden är normenlig finns det inga nackdelar med att skarva armeringen inom hörnområdet i ett hörn belastat med stängande moment.

Nyckelord: Armerad betong, vidhäftning, spjälkande effekter, tredimensionell analys, utdragsförsök, cyklisk last, finita element-analys, ickelinjär brottmekanik, skarvning av armering.

LIST OF PUBLICATIONS

This thesis is based on the work contained in the following papers, referred to by Roman numerals in the text:

I   "Modelling Splitting and Fatigue Effects of Bond", in *Fracture Mechanics of Concrete Structures Proceedings* FRAMCOS-3, AEDIFICATIO Publishers, D-79104 Freiburg, Germany, 1998, pp. 675—685. (Co-author: K. Gylltoft).

II   "Pull-out Tests of Steel-Encased Specimens Subjected to Reversed Cyclic Loading", submitted to *Materials and Structures*.

III   "Bond Modelling in Three-Dimensional Finite Element Analyses", in July 1999 provisionally accepted for publication in *Magazine of Concrete Research*. (Co-author: K. Gylltoft).

IV   "Static Tests and Analyses of Frame Corners Subjected to Closing Moments", submitted to *Journal of Structural Engineering*.

CONTENTS

PREFACE

In this study, a theoretical model of the bond action in reinforced concrete was developed and used in finite element analyses of pull-out tests and frame corners. Pull-out tests and tests on frame corners were also carried out. Most of the work was done between January 1996 and November 1999. This work is part of a research project, "Detailing of frame corners in concrete bridges", which extended from July 1996 to June 1999, at the Division of Concrete Structures, Chalmers University of Technology. The research project was financed by the Swedish Council for Building Research (BFR), the Development Fund of the Swedish Construction Industry (SBUF), and the Swedish Road Administration (Vägverket). The work has been followed by a reference group consisting of representatives from the building industry and from the Swedish Road Administration. Their interest and valuable comments are hereby acknowledged.

I am most grateful to my supervisor, Professor Kent Gylltoft, for his guidance, support, valuable discussions and encouragement. I also thank Professor Björn Engström, who was my supervisor during my first period as a doctoral student, for his support and valuable discussions, and Professor Emeritus Krister Cederwall, my office mate, for his encouragement.

I am also most grateful to all of the doctoral students at the Division of Concrete Structures for much support, many discussions and the good times we have had together. In particular, I would like to thank Jonas Magnusson and Morgan Johansson for many interesting discussions about bond and frame corners. All of the tests were carried out in the laboratory of the Department of Structural Engineering at Chalmers University of Technology. The laboratory staff is remembered with appreciation for technical assistance during the experiments. Lars Wahlström made the photographs for this thesis, and Wanda Sobko produced some of the figures. I thank also Yvonne Juliusson for all assistance, and Lora Sharp-McQueen for improving the language in most of the thesis. I enjoyed working with Ken Olausson and Carina Haga, who did their degree project as a part of the larger research project.

Finally, special thanks go to my family, Stefan, Martin and Thomas Lundgren, for their love and support.

Göteborg, November 1999

Karin Lundgren

NOTATIONS

CAPITAL LETTERS

A	area
A'	area of one rib
$\mathbf{D}$	elastic stiffness matrix
D_{11}	stiffness in the elastic stiffness matrix
D_{12}	stiffness in the elastic stiffness matrix
D_{22}	stiffness in the elastic stiffness matrix
E_c	modulus of elasticity of concrete
F	force
F_1	yield line describing the friction
F_2	yield line describing the upper limit at a pull-out failure
G	plastic potential function
G_F	fracture energy of concrete
L^d	length of damaged zone

LOWER CASE LETTERS

c	parameter in yield function F_2 (in the second version of the model the stress in the inclined compressive struts)
d	diameter
f_{cc}	compressive strength of concrete
f_{ct}	tensile strength of concrete
l	length
l_k	distance between ribs
r	radius
r_a	inner radius
r_b	outer radius
$\mathbf{t}$	the tractions at the interface
t_n	normal splitting stress
t_{n0}	apex of the yield lines in the first version of the model
t_t	bond stress

$\mathbf{u}$	the relative displacements across the interface
u_n	relative normal displacement at the interface
u_n^{e}	elastic part of the relative normal displacement at the interface
u_n^{p}	plastic part of the relative normal displacement at the interface
u_t	slip
u_t^{e}	elastic part of the slip
u_t^{p}	plastic part of the slip
u_{tmax}	maximum value of the slip which has been obtained
u_{tmin}	minimum value of the slip which has been obtained

GREEK LOWER CASE LETTERS

η	parameter in the plastic potential function G
η_d	the parameter η in the damaged deformation zone
η_{d0}	the lowest value of the parameter η_d in the damaged deformation zone
κ	hardening parameter
λ	plastic multiplier
μ	coefficient of friction
μ_d	the coefficient of friction in the damaged deformation zone
μ_{d0}	the lowest value of the coefficient of friction in the damaged deformation zone
μ_{max}	maximum coefficient of friction
υ	the Poisson ratio

1 INTRODUCTION

1.1 Background, Aim and Scope

The bond mechanism between deformed bars and concrete has been investigated by numerous researchers. While it is known to be influenced by many parameters, the most important are the confinement of the surrounding structure and yielding of the reinforcement. However, when reinforced concrete structures are modelled with finite element analysis, it is quite common to assume that the bond stress depends solely on the slip. The confinement of the surrounding structure must then be evaluated before the analysis can be started, in order to choose an appropriate bond-slip correlation as input. Whether the reinforcement will yield or not must also be known in advance, for the same reason. The goal of this project was to design a general model of the bond mechanism for which the same set of input parameters can be used in all cases; here, the bond-slip is a result of an analysis, rather than input. It was then intended to use the model in analyses of spliced frame corners.

Until recently, splicing of the reinforcement in frame corners had not been allowed by the Swedish Road Administration. This had led to complicated reinforcement layouts that were hard to realise on site. It was therefore of interest to study how splicing the reinforcement within the corner region affects the behaviour of a structure. The bends of the reinforcement bars in the corners cause splitting stresses. When the reinforcement is spliced, additional splitting stresses arising from the anchorage of the reinforcement could cause a decreased bond capacity. By using detailed three-dimensional models combined with a suitable model for the bond, these effects could be taken into account in analyses.

1.2 Limitations

The goal here was to develop a general model of the bond mechanism to be used in detailed finite element analyses of concrete structures. When such analyses are conducted, suitable material models for the concrete are of course needed. The material models used are the ones available in the finite element program DIANA, see TNO (1998). The results of the analyses showed that sometimes the material model

used was not sufficient to describe the behaviour accurately. This applied, for example, to the analyses in which the concrete was exposed to cyclic loading or to a triaxial stress state. The improvement of material models is, however, outside the scope of this thesis.

For the tests and analyses of frame corners to investigate the effect of splices, the study has been limited to closing moments. The reason for this was that the effect of opening moments has been studied more extensively by other researchers already.

1.3   Outline of Contents

This thesis consists of four papers and this introductory part. An introduction to selected topics is given in the first part: Non-linear fracture mechanics is briefly presented in Chapter 2, the bond mechanism and related models are outlined in Chapter 3, and the structural behaviour of frame corners is discussed in Chapter 5. The new work is presented mainly in the papers. The work started with the design of a new model for the bond mechanism between reinforcement bars and concrete. This model and analyses of some pull-out tests are described in Paper I. Since there was a lack of experimental data on how the splitting stresses are affected by cyclic loading, pull-out tests on steel-encased concrete cylinders were carried out; these are presented in Paper II. The results of these tests revealed some drawbacks to the model which was then changed accordingly. The alteration of the model, with reasons for changes, is presented in Chapter 4. The second version of the model is presented in Paper III, together with analyses of pull-out tests, specially chosen to describe various types of failure. Finally, the model was used in three-dimensional analyses of frame corners, and the results therefrom are compared with results from experiments in Paper IV.

1.4   Original Features

A new theoretical model of the bond mechanism in monotonic and cyclic loading was developed. The fundamentals of the model are the friction between the reinforcement bar and the concrete, as well as the limitation of the stresses in the inclined compressive forces that result from the bond action. This way of describing the bond mechanism as a combination of basic mechanisms and combining them in an elasto-plastic model has not, to the author's knowledge, been tried before. Furthermore,

tests, as well as finite element analyses of pull-out tests and frame corners were conducted. The steel-encased pull-out tests with specimens subjected to cyclic loading are believed to be unique, since no tests have been found in the literature that show the effect of the splitting stresses measured during cyclic loading.

2   NON-LINEAR FRACTURE MECHANICS FOR CONCRETE STRUCTURES

2.1   Tensile Behaviour

Since the fictitious crack model was presented by Hillerborg *et al.* (1976), and the crack band theory by Bažant and Oh (1983), non-linear fracture mechanics for concrete structures has been extended and used by many researchers. A brief overview of the subject is given here. For more information, see for example Jirásek (1999).

The two basic ideas of non-linear fracture mechanics are that some tensile stress can continue to be transferred after microcracking has started, and that this tensile stress depends on the crack opening, which is a displacement, rather than on the strain (as it does in the elastic region), see Figure 1. The area under the tensile stress versus crack opening curve equals an energy which is denoted the fracture energy, G_F. This is assumed to be a material parameter.
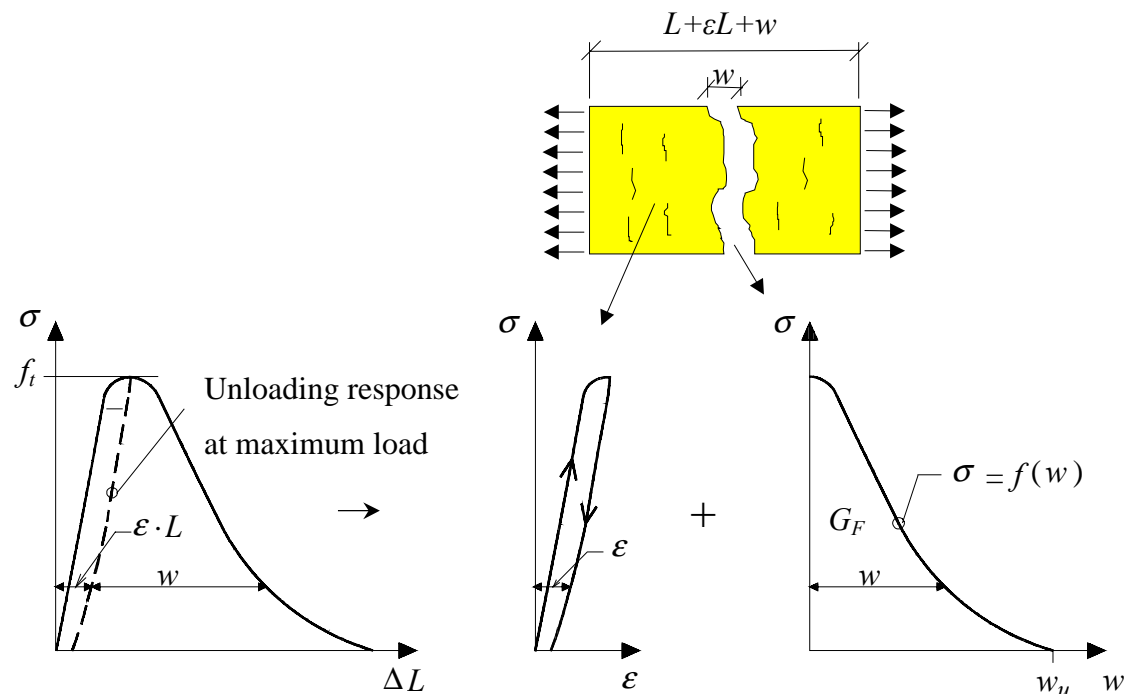
Figure 1   Mean stress-displacement relation for a uniaxial tensile test specimen, subdivided into a general stress-strain relation and a stress-displacement relation for the additional localised deformations.

From the first models, that used discrete crack elements, the smeared approach was devised. This means that the deformation of one crack is smeared out over a characteristic length. When modelling plain concrete, or when slip is allowed between the reinforcement and the concrete, this characteristic length is approximately the size of one element. This means that the tensile stress versus strain used will depend on the size of the element. For axisymmetric analyses, the characteristic length depends on the number of radial cracks assumed. The more radial cracks that are assumed, the smaller the characteristic length will be, see Figure 2. When modelling reinforced concrete and assuming complete interaction between the steel and the concrete, the deformation of one crack is smeared out over the mean crack distance.

In the first models that used the smeared approach, the direction of the cracks was fixed. Special input was required in order to determine how large the shear stresses were that could continue to be transferred across a crack. Several cracks could develop within the same element. There was, however, a certain threshold angle, that specified the minimum angle between two cracks. The transfer of shear stresses across a crack, combined with this threshold angle, allowed the tensile stresses in the material to exceed the tensile strength, as long as the direction of the tensile stress was close enough to an already formed crack. In particular, when the direction of the principal stress changes after cracking, there can be large tensile stresses.
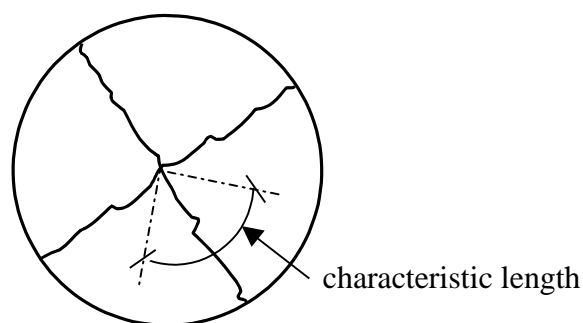
Figure 2   Characteristic length in axisymmetric models.

To avoid these large stresses, rotating crack models were developed. In these models, the direction of a crack is not fixed, but rotates with the direction of the maximum tensile strain. Generally, coaxiality between principal stresses and principal strains is assumed. The special input for the shear stresses across the crack is no longer needed, since these stresses become zero by definition. The behaviour of the rotating crack models is rather close to elasto-plastic models that have been worked out and used, for example the Rankine criterion that limits the maximum tensile stress.

After the smeared approach, the concept of embedded crack models was evolved, see for example Åkesson (1996). Here, the crack is modelled as a strain localisation within an element. This approach has the benefit of not needing any characteristic length as input. However, since no three-dimensional model was available when this project started, the smeared approach was chosen for the analyses.

As mentioned, the smeared approach needs a characteristic length as input. There are some problems in choosing the characteristic length that arise almost immediately when modelling reinforced concrete structures. Some examples that have appeared during this work are discussed here. Since slip was allowed between the reinforcement and the concrete in the analyses carried out, this characteristic length should be related to the size of one element. However, this is a problem when the dimensions of the elements are not the same in all directions. If the crack pattern is known before the analysis is carried out, the most accurate assumption would be to use the size of the element perpendicular to the crack plane, see Figure 3. If, however, the crack pattern is not known in advance, or when cracks appear in more than one direction in an element, a mean value is usually used. This means that the ductility of the concrete in one direction is overestimated (the length of the elements), and in another direction underestimated (the width of the elements).
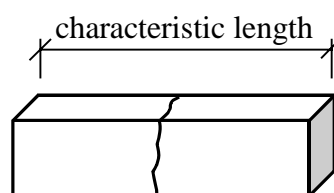
Figure 3   Characteristic length in oblong elements.

The easiest and simplest solution to this problem is of course to use meshes in which the elements have about the same size in all directions. However, there can also be problems in doing this. In the three-dimensional analyses of frame corners presented in Paper IV, the mesh had to be adjusted to fit around the main reinforcement bar. This means that the smallest dimension of an element had to be as small as about 4 mm. If this size had also been chosen for the dimension in the direction along the reinforcement bar, the number of elements needed to model the corner region would have become very large, and the time required for the analysis would not have been reasonable. Furthermore, another problem was that slip between the main reinforcement and the concrete was accounted for, while the transverse reinforcement was modelled with complete interaction. These problems were solved (by good fortune more than skill); the characteristic length was chosen as the length of the elements along the main reinforcement bars and the splitting cracks localised in two elements instead of in one, see Figure 11 in Paper III and Figure 14 in Paper IV. Thus, the characteristic length chosen was rather realistic for cracks in both directions.

2.1   Compressive Behaviour

Since cracks are easy to spot, localisation of the deformations in a tensile failure of concrete is not difficult to understand. However, there is also localisation of the deformations in a compressive failure. Van Mier (1984) showed that the compression softening behaviour is related to the boundary conditions and the size of the specimen. An explanation could be that the lateral deformations are partly restrained at the supports, even though brushes were used to reduce the frictional restraint at the end-zones. However, these effects are most likely partly due to localisation of the deformations in a compressive failure, see Figure 4. This has been confirmed in a Round Robin Test, see van Mier *et al.* (1997). Markeset (1993) has presented a model for this, see Figure 5. One of the parameters of the model was the length of the damaged zone, L^d, shown in the figure. It was assumed to be about 2.5 times the smallest lateral dimension for centric compressed specimens. When strain gradients were present, it was assumed to depend on the depth of the damaged zone. Reinforcement probably affects the length of the damaged zone also.
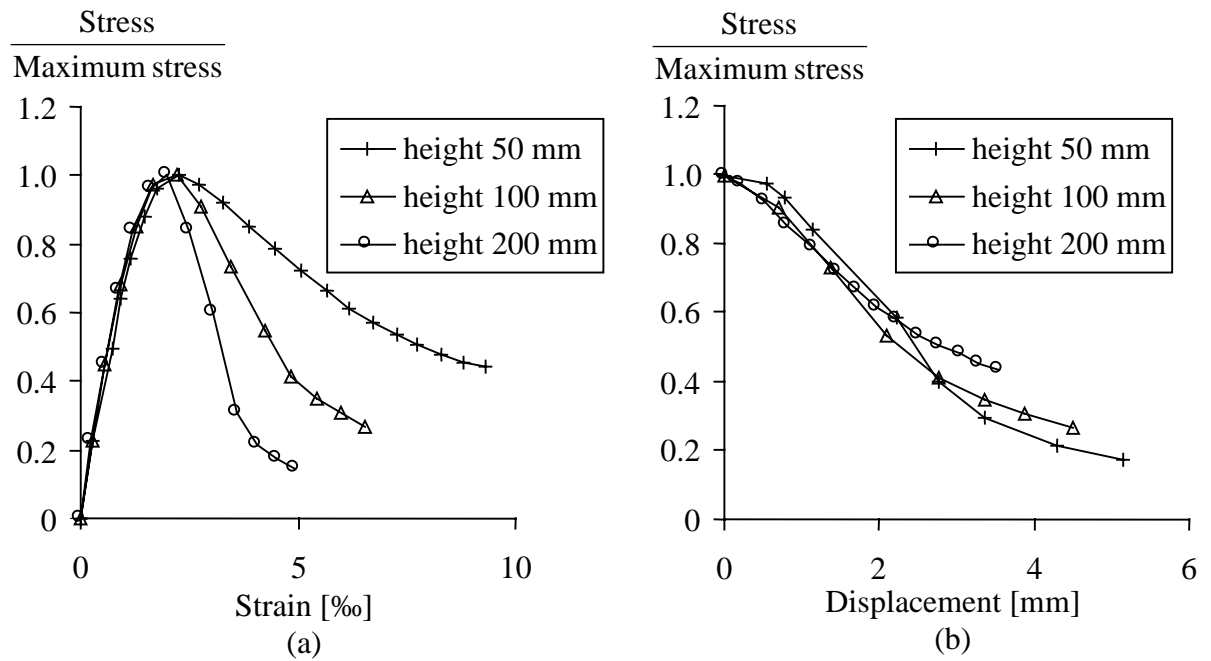
Figure 4   Results from uniaxial compressive tests by van Mier (1984): (a) Stress versus strain, and (b) Post-peak stress versus displacement for various specimen heights.
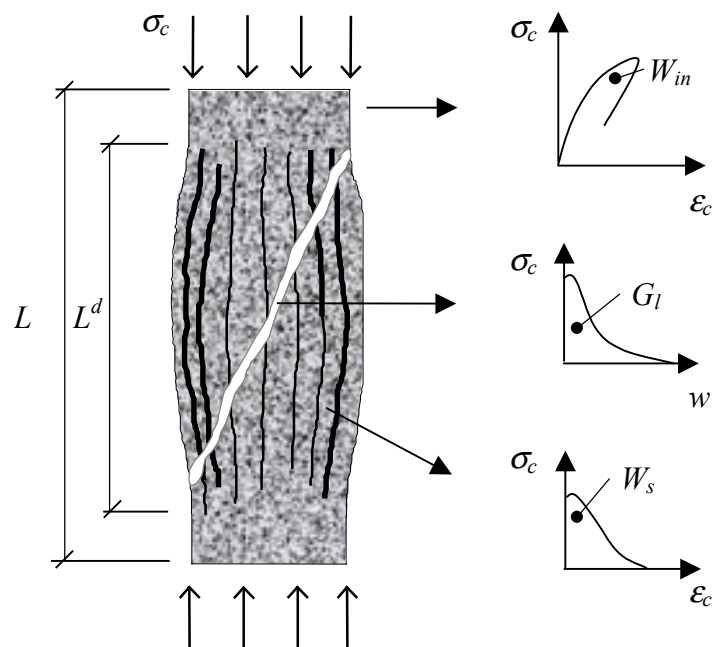
Figure 5   Illustration of the model developed by Markeset (1993) for a specimen loaded in uniaxial compression.

The model by Markeset (1993) can serve as a tool for analyses of beams and columns with uniaxial compression. However, there is at present no convenient way to take the effect of localisation into account in a generalised material model suited for finite element analysis, especially not for a general case with triaxial stress states. One problem is that the number of elements in which the compressive region will localise is not known when the analysis is started. While in tension, it seems reasonable to assume that a crack will localise in one element, an assumption that is not so obvious for compression. In the analyses presented in this thesis, simple stress versus strain relations for the compressive behaviour were used without taking into account the size of the elements.

3 BOND BETWEEN REINFORCEMENT AND CONCRETE

3.1 The Bond Mechanism

The bond mechanism is the interaction between reinforcement and concrete. It is this transfer of stresses that makes it possible to combine the compressive strength of the concrete and the tensile capacity of the reinforcement in reinforced concrete structures. Thus, the bond mechanism has a strong influence on the fundamental behaviour of a structure, for example in crack development and spacing, crack width, and ductility.

3.1.1 Monotonic loading

The bond mechanism is considered to be a result of three different mechanisms: chemical adhesion, friction, and mechanical interlocking between the ribs of the reinforcement bars and the concrete, see Figure 6. This statement can be found in, for example, ACI (1992). However, the mechanical interlocking can be viewed as friction, depending on the level at which the mechanism is considered. The bond resistance resulting from the chemical adhesion is small; it is lost almost immediately when slipping between the reinforcement and the concrete starts, ACI (1992), CEB (1982). The inclined forces resulting from the bearing action of the ribs make it possible, however, to continue to transfer forces between the reinforcement and the concrete. This implies that bond action generates inclined forces which radiate outwards in the concrete. The inclined stress is often divided into a longitudinal component, denoted the bond stress, and a radial component, denoted normal stress or splitting stress, see Figure 7.

（a) Adhesion   (b) Friction   (c) Bearing
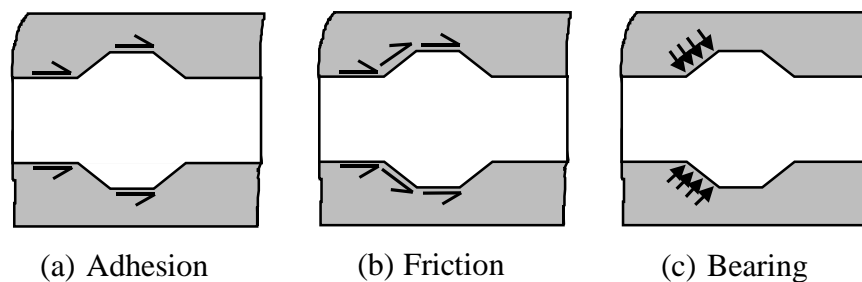
Figure 6   Idealised force transfer mechanisms, modified from ACI (1992).

(a) Stress on the
reinforcing bar

(b) Stress on the concrete
and its components
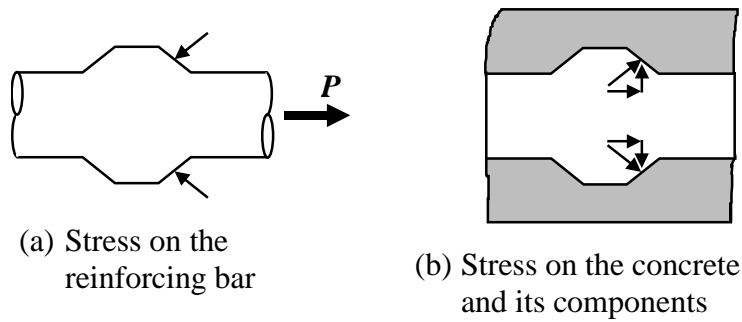
Figure 7   Bond and splitting stresses between a deformed bar and the surrounding
concrete. From Magnusson (1997).

The inclined forces are balanced by ring tensile stresses in the surrounding concrete, as explained by Tepfers (1973), see Figure 8. If the tensile stress becomes large enough, longitudinal splitting cracks will form in the concrete. Another type of crack that is directly related to the bond action are the transverse microcracks which originate at the tips of the ribs, Goto (1971), see Figure 9. These cracks are due to the local pressure in front of the ribs, which gives rise to tensile stresses at the tips of the ribs. These transverse microcracks are also called bond cracks.

Splitting crack
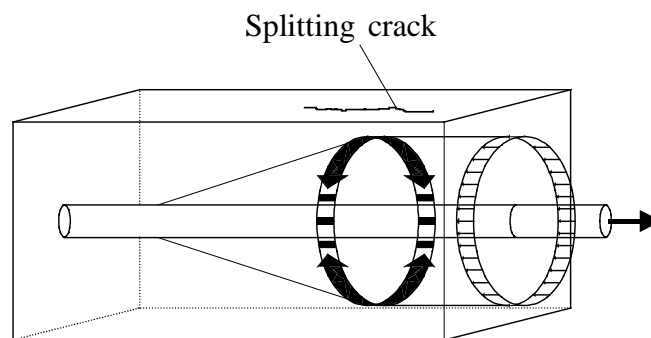
Figure 8   Ring tensile stresses in the anchorage zone, according to Tepfers (1973).
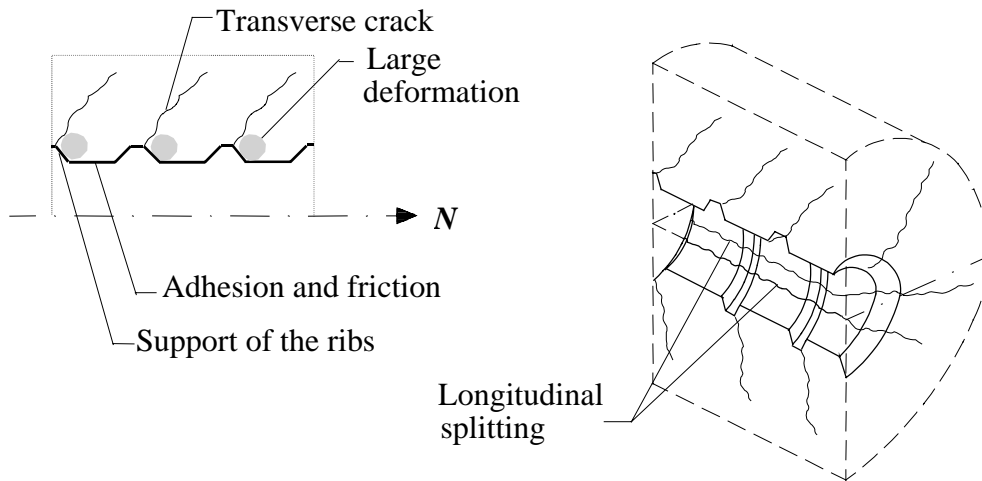
Figure 9   Deformation zones and cracking caused by bond, modified by Magnusson (1997) from Vandewalle (1992).

It should be noted that the presence of the normal stresses is a condition for transferring bond stresses after the chemical adhesion is lost. When, for some reason, the normal stresses are lost, bond stresses cannot be transferred. This is what happens if the concrete around the reinforcement bar is penetrated by longitudinal splitting cracks, and there is no transverse reinforcement that can continue to carry the forces. This type of failure is called splitting failure. The same thing happens if the reinforcement bar starts yielding. Due to the Poisson effect, the contraction of the steel bar increases drastically at yielding. Thus, the normal stress between the concrete and the steel is reduced so that only low bond stress can be transferred.

When the concrete surrounding the reinforcement bar is well-confined, meaning that it can withstand the normal splitting stresses, and the reinforcement does not start yielding, a pull-out failure is obtained. When this happens, the failure is characterised by shear cracking between two adjacent ribs. This is the upper limit of the bond capacity.

A common way to describe the bond behaviour is by relating the bond stress to the slip, that is the relative difference in movement between the reinforcement bar and the concrete. As made clear above, the bond versus slip relationship is not a material parameter; it is closely related to the structure. It also depends on several parameters such as casting position, vibration of the concrete and loading rate. Examples of schematic bond-slip relationships are shown in Figure 10.
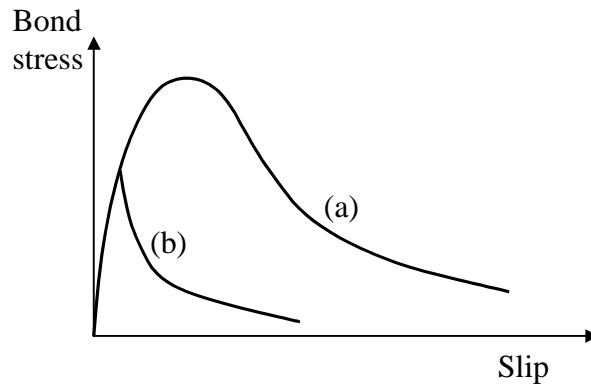
Figure 10   Schematic bond-slip relationship: (a) pull-out failure; (b) splitting failure, or loss of bond due to yielding of the reinforcement.

3.1.2   Cyclic loading

A typical response for bond in cyclic loading is shown in a bond versus slip diagram in Figure 11. The monotonic curve is followed for the first loading until point A in the figure. Thereafter occurs a steep unloading to point B, and then an almost constant, low bond stress until the original monotonic curve is reached at point C. As for monotonic loading, the response depends on the structure, and the influencing parameters are the same. Moreover, the response is also influenced by the type of cyclic loading. According to ACI (1992), load cycles with reversed loading cause a greater degradation of bond strength and stiffness than the same number of load cycles with unidirectional loading. The peak value of the slip is a critical factor. Additional cycles between slip values smaller than earlier ones do not significantly influence the bond behaviour, according to Eligehausen *et al*. (1983), Balázs (1991) and ACI (1992).
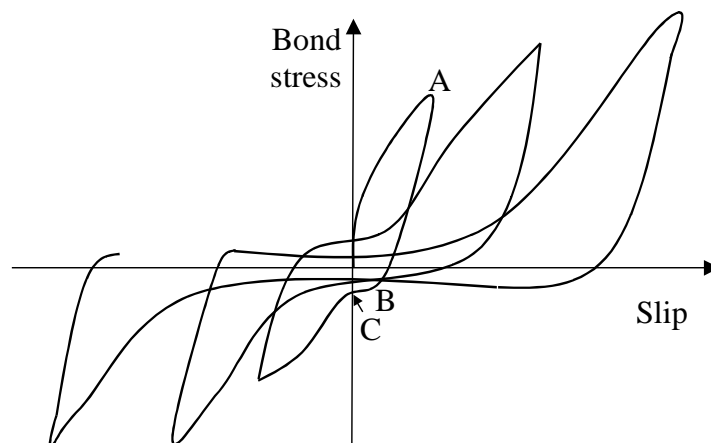
Figure 11   Typical bond versus slip for cyclic loading.

3.2 Steel-Encased Pull-Out Tests Subjected to Reversed Cyclic Loading

As discussed in Section 3.1.1, anchoring deformed bars in concrete gives rise not only to bond stresses but also to splitting stresses. Although many experiments have been conducted to study the bond stresses, the splitting stresses are less investigated. Tepfers and Olsson (1992) have done "ring tests" in which a reinforcement bar was pulled out of a concrete cylinder surrounded by a thin steel tube. By measuring the tangential strains in the steel tube, the splitting stresses could be evaluated. A few other researchers have also carried out tests to find solutions to the problems of measuring the splitting stresses, for example Malvar (1992). The effect on bond of cyclic loading has been investigated by, among others, Eligehausen *et al*. (1983) and Balázs and Koch (1995), who have conducted large programmes of pull-out tests with cyclically loaded specimens. However, no tests were found in the literature that show the effect of the splitting stresses measured during cyclic loading.

Therefore, steel-encased pull-out tests subjected to reversed cyclic loading were carried out, see Paper II or Lundgren (1998). The main purpose of these tests was to give reference information for calibrating models of the bond mechanism, to improve knowledge of the splitting stresses, and to investigate how they are affected by reversed cyclic loading. Hence, a reinforcement bar was pulled out of a concrete cylinder surrounded by a thin steel tube. The effect of the splitting stresses during cyclic loading could be studied by measuring the tangential strains in the steel tube, together with the applied load and slip. In five tests, specimens were loaded by monotonically increasing the load, while nine other tests subjected specimens to reversed cyclic loading. All of the tests resulted in pull-out failures. The results from the monotonic tests indicate that the splitting stresses decreased after the maximum load had been obtained, although not as much as the load decreased. The results from the cyclic tests show a typical response for bond in cyclic loading. When there was almost no bond capacity left, the measured strain in the steel tubes stabilised and remained more or less unaffected by the last load cycles. The test results provided valuable information which influenced not only the calibration of the bond model but also the formulation of the model; more detail is given in Section 4.2.

3.3 Theoretical Models of the Bond Mechanism

When reinforced concrete structures are analysed, complete interaction between the reinforcement and the concrete is perhaps the most frequent assumption. This assumption is used in almost all hand calculations, for example in the analytical models for bending moment in the ultimate limit state. In finite element analyses also, this is a rather commonly used assumption; especially when the overall behaviour of a larger structure is examined, this assumption is often sufficient for the level of modelling desired.

Nevertheless, for more detailed analyses of smaller parts of a structure, especially if one is interested in following the crack development more thoroughly, the bond mechanism needs to be taken into account. The most usual way to do this is to employ bond versus slip relations as input. Several researchers have examined the bond mechanism and suggested various bond versus slip curves to be used in analyses, for example Tassios (1979), and Eligehausen *et al.* (1983) include both monotonic and cyclic loading. However, as discussed in Section 3.1.1, the bond versus slip depends on the structure. As long as this is kept in mind, a reasonable bond versus slip relation can be assumed by taking parameters such as the actual concrete cover, the amount of transverse reinforcement *etc*. into account. If one wishes to study crack development in structural members for example, then this way of taking the bond mechanism into account offers a sufficient level of accuracy and detail.

However, for more detailed analyses of parts of a structural member where the bond mechanism plays a decisive role for the behaviour, a more refined model for the bond is needed. This is needed mainly for analyses of anchorage regions, such as in splices and anchorage of the reinforcement at end supports, but also for analysis of the rotational capacity, where the bond plays a crucial part. A requirement for this type of model is that the bond mechanism be described in such a way that the bond versus slip achieved in a structure is a result of the analysis, rather than input. Another requirement is that the model includes not only the bond stresses, but also the splitting stresses that result from the anchorage.

The model by Gylltoft (1983) included the effect of normal stresses, which allows an outer pressure to increase the capacity. Furthermore, the model could deal with cyclic loading; fracture mechanics was used to describe the damage. However, the model did

not include any active normal splitting stresses that result from the anchorage, and bond versus slip was used for the input.

Some models that include the active splitting stresses, while still using a form of bond versus slip as input, have been developed, see for example Mainz (1993). Also, some attempts to model the bond mechanism in a more thorough way by including the ribs of the reinforcement in the geometrical model have been done, for example by Reinhardt *et al.* (1984). The model by den Uijl and Bigaj (1996), see also Bigaj (1999), includes the splitting stress; the bond stress is related not only to the slip, but also to the radial deformation between the reinforcement bar and the concrete. The model can therefore describe the loss of bond if the reinforcement yields. This is an analytical model, for which the effect of the confinement is obtained from analyses of a thick-walled cylinder. The results of the model show good agreement with test results. This model can serve as a valuable tool for getting information about what bond versus slip should be used as input in an analysis of a structure. However, it does not seem possible to implement it in a more general way, for example in a finite element program. Hence, if a part of a structure is to be modelled, some results of the analysis need to be known in advance, such as whether splitting failure will occur.

The model by Åkesson (1993) and the one by Cox (1994) represent a new kind of model. In these models, the splitting stresses are included, and the bond stress depends not only on the slip but also on the radial deformation between the reinforcement bar and the concrete. This makes it possible to include the effect of the confinement of the surrounding structure. Both models use elasto-plastic theory, as shown by the yield lines in Figure 12.
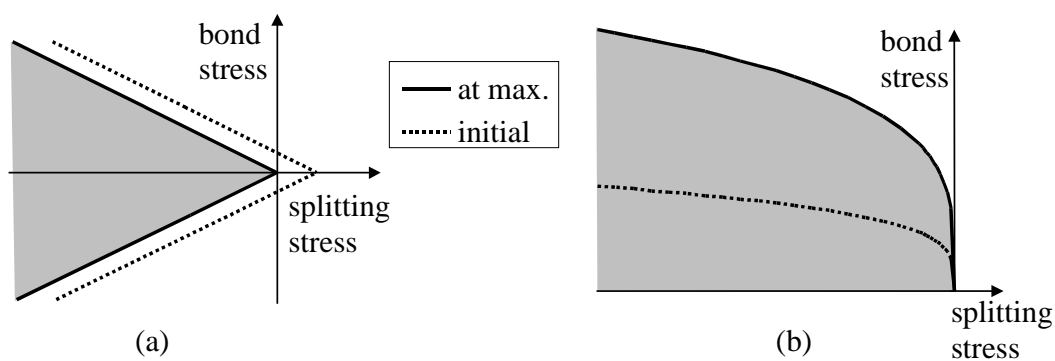
Figure 12   Yield lines of the models of (a) Åkesson (1993) and (b) Cox (1994).

In Åkesson's model, the yield line describes the friction with adhesion included. The adhesion is assumed to decrease to zero for relatively small slip. This model was devised for studies of the release of prestressed strands in hollow core slabs. It was therefore intended to be used only for monotonic loads.

To limit the bond capacity, Åkesson made the elastic stiffness describing the relation between the normal stress and the slip non-linear, with a maximum followed by decreasing normal stress. This gives reasonable results for monotonic loading. For cyclic loading, however, it can give unexpected results, such as that the normal stress increases at unloading. Note, however, that the model was not intended for cyclic loading.

Another drawback to Åkesson's model is that there is no upper limit of the bond stress prescribed by the yield lines; as can be seen in Figure 12 (a), the bond stress can become infinitely high as long as enough normal stress is present. This does not agree with the experimental results of, for example, Robins and Standish (1984). Their tests showed that lateral confinement changed the failure mode from splitting failure to pull-out failure. Yet, further increase of the lateral confinement had no effect on the bond capacity. However, outer pressure was outside the scope of the model.

The model by Cox (1994) does not have this drawback; as can be seen in Figure 12 (b), the bond stress curves towards an upper limit when the normal stress increases. The initial increase followed by a decrease in bond stress (compare with the bond versus slip curves in Figure 10) is obtained in this model by letting the yield surface harden, as shown in Figure 12 (b), and thereafter soften almost to the initial yield line again. This model is probably a more general model of the bond mechanism than the model by Åkesson. Still, it has not been shown to describe the loss of bond when the reinforcement yields. Furthermore, it seemed entirely possible that the physical behaviour could be described in a more fundamental way.

4   A NEW BOND MODEL

4.1   Presentation of a New Bond Model

A new bond model which includes the splitting stresses was developed. With one set of input parameters, this new model produces different bond-slip curves, determined by the confinement of the surrounding structure and whether or not the reinforcement is yielding. The effect of cyclic loading with varying slip direction is also important for the bond resistance, which is why this effect was included in the model. The model was implemented in the finite element program DIANA, for more detail see Lundgren (1999a). In DIANA, there are interface elements available, which describe a relation between the tractions **t** and the relative displacements **u** at the interface. These elements are used at the surface between the reinforcement bars and the concrete. The physical interpretations of the variables t_n, t_t, u_n and u_t are shown in Figure 13. The interface elements have, initially, a thickness of zero.

$$\mathbf{t} = \begin{bmatrix} t_n \\ t_t \end{bmatrix} = \begin{bmatrix} \text{normal splitting stress} \\ \text{bond stress} \end{bmatrix}$$

$$\mathbf{u} = \begin{bmatrix} u_n \\ u_t \end{bmatrix} = \begin{bmatrix} \text{relative normal displacement at the layer} \\ \text{slip} \end{bmatrix}$$
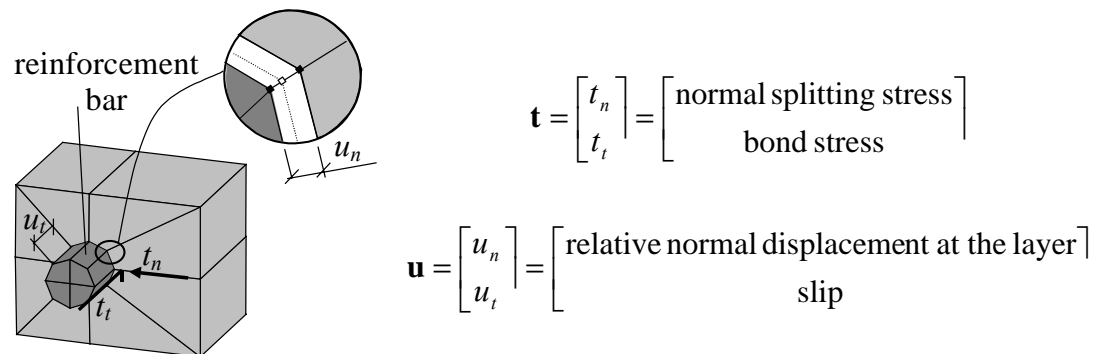
Figure 13   Physical interpretation of the variables t_n, t_t, u_n and u_t.

4.1.1 Elasto-plastic formulation

The new bond model is a frictional one, using elasto-plastic theory to describe the relations between the stresses and the deformations. Thus, the model has yield lines, flow rules, and hardening laws. The relation between the tractions **t** and the relative displacements **u** is in the elastic range:

$$\begin{bmatrix} t_n \\ t_t \end{bmatrix} = \begin{bmatrix} D_{11} & \dfrac{|u_t|}{u_t} D_{12} \\ 0 & D_{22} \end{bmatrix} \begin{bmatrix} u_n \\ u_t \end{bmatrix} \tag{1}$$

where D_{12} is normally negative, meaning that slip in either direction will cause negative t_n, i.e. compressive forces radiating outwards. The yield lines are described by two yield functions, one for the friction, F_1, assuming that the adhesion is negligible:

$$F_1 = |t_t| + \mu t_n = 0. \tag{2}$$

The other yield line, F_2, describes the upper limit for a pull-out failure. This is determined from the stress in the inclined compressive struts that result from the bond action, see Figure 14.

$$F_2 = t_t^2 + t_n^2 + c \cdot t_n = 0 \tag{3}$$

Equilibrium gives:

$$\sqrt{t_t^2 + t_n^2} \cdot dl \cdot rd\varphi = c \cdot dl \sin\alpha \cdot rd\varphi$$

$$\sin\alpha = \frac{-t_n}{\sqrt{t_t^2 + t_n^2}}$$

$$t_t^2 + t_n^2 + c \cdot t_n = 0$$
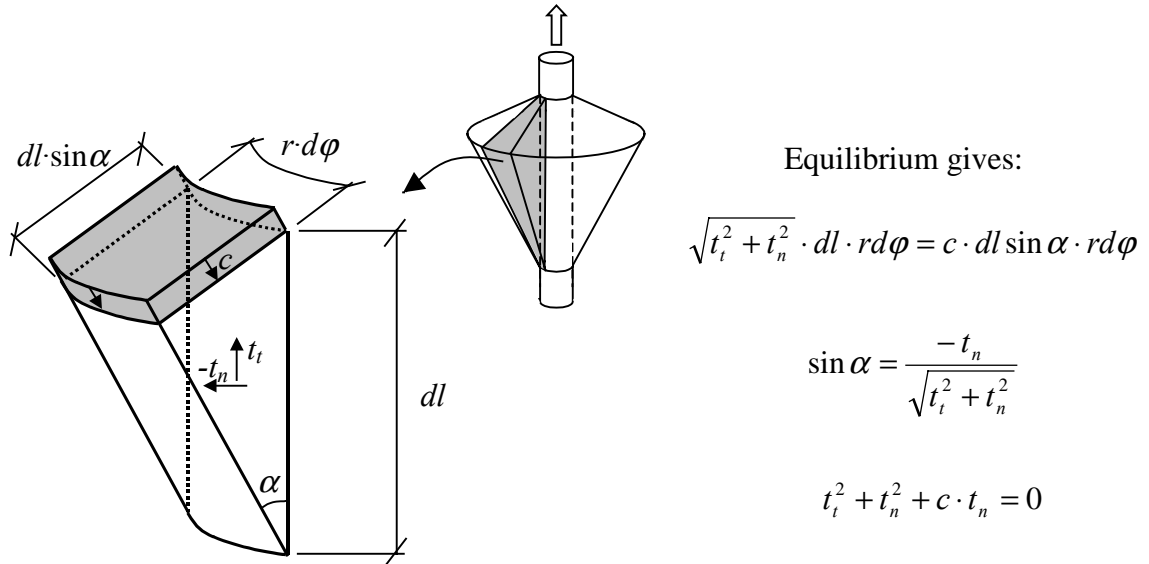
Figure 14   The stress in the inclined compressive struts determines the upper limit.

For plastic loading along the yield line describing the upper limit, F_2, an associated flow rule is assumed. For the yield line describing the friction, F_1, a non-associated flow rule is assumed, for which the plastic part of the deformations is

$$d\mathbf{u}^\mathbf{p} = d\lambda \frac{\partial G}{\partial \mathbf{t}}, \qquad G = \frac{|u_t|}{u_t} t_t + \eta t_n = 0 \tag{4}$$

where $d\lambda$ is the incremental plastic multiplier. The yield lines, together with the direction of the plastic part of the deformations, are shown in Figure 15. At the corners, a combination of the two flow rules is used; this is known as the Koiter rule.

For the hardening law of the model, a hardening parameter κ is established. It is defined by

$$d\kappa = \sqrt{du_n^{p\,2} + du_t^{p\,2}} \; . \tag{5}$$

The variables μ and c in the yield functions are assumed to be functions of κ.
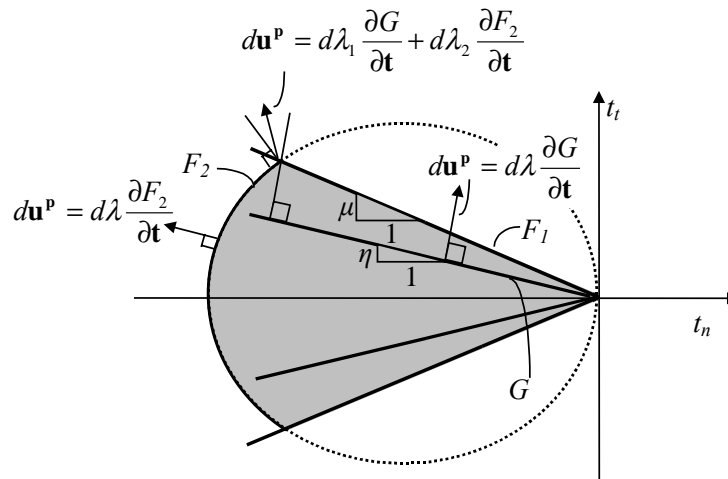
Figure 15 The yield lines. The plastic part of the deformations, $d\mathbf{u}^\mathbf{p}$, is given by an associated flow rule at the yield line describing the upper limit, F_2, and a non-associated flow rule at the yield line describing the friction, F_1.

4.1.2 Damaged and undamaged deformation zones

A typical response for bond with varying slip direction is a steep unloading and then an almost constant low bond stress until the original monotonic curve is reached; this is described in Section 3.1.2. To make the model describe this typical response, a new concept, called *damaged and undamaged deformation zones*, is used. The idea is that when the reinforcement slips in the concrete, the friction will be damaged (reduced) in the range of the passed slip. This is a simplified way to describe the damage of the cracked and crushed concrete. In Figure 16 (b), the reinforcement is back in its original position after slipping in both directions. The concrete, consequently, is crushed in the range of the passed slip. While this crushed concrete still has some capacity to carry compressive load, it has no capacity at all in tension. The friction is therefore assumed to vary in the damaged zone, depending on whether loading is applied in the direction away from, or towards, the original position, as shown in Figure 16 (c) and (d). It is assumed to drop immediately to a low value, μ_{d0}, at load reversal, and to keep this value until the original position is reached. For further loading, away from the original position, the friction is assumed to increase gradually until the undamaged zone is reached and the normal value of μ is used again. To describe this gradual increase, an equation of the second degree has been chosen.

The parameter η also has a lower value in the damaged deformation zone, varying in the same way as just described for the coefficient of friction. This lower value corresponds physically to the fact that the increase in the stresses is lower in the damaged than in the undamaged deformation zone.
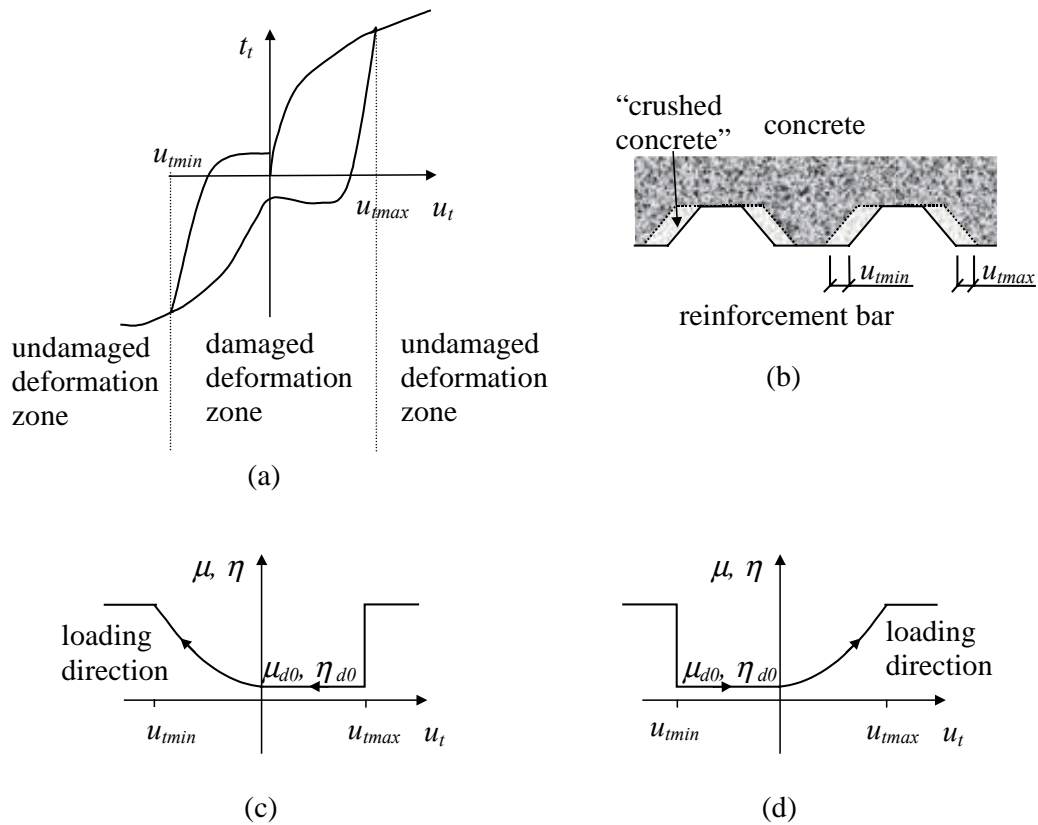
Figure 16   (a) One load cycle with varying slip directions. (b) The reinforcement bar is back in its original position, after slipping in both directions. Maximum and minimum values of the slip are marked. (c) and (d) The parameters μ and η vary within the damaged deformation zone depending on whether the loading is directed towards or away from the original position.

4.2   Development of the Bond Model

The bond model described in the previous section is the same as that presented in Paper III. In Paper I, an earlier version of this model is described. The two versions are slightly different: the one in Paper III can be viewed as an improvement of the first one. The main reason for the changes was the results from the steel-encased pull-out tests that are reported in Paper II. Sections 4.2.1 through 4.2.4 cover the differences between the two versions of the models with reasons for the changes.

4.2.1   The yield line describing the upper limit

In both versions of the model, the yield lines are two yield functions, one describing the friction and the other describing the upper limit of a pull-out failure. In the first version of the model, little attention was paid to the formulation of the upper limit. Only one example was considered: the theoretical one with zero bond stress, which leads to a limit of the splitting stress about the same as the compressive strength of the concrete. By examining the results from pull-out tests, a reasonably large bond capacity was then obtained simply by setting an upper limit with straight lines, as shown in Figure 17.

In the second version of the model, the combinations of splitting stresses and bond stresses were recognised as inclined compressive struts. By letting the stress in these compressive struts be limiting, a new expression was derived for the upper limit, see Figure 14. This new expression is believed to be better than the first one, since it corresponds more closely to the physical reality. When results from analyses were compared with results from the monotonically loaded steel-encased pull-out tests, it also appeared that the second version of the model gave improved results. The main drawback to the first version of the model was that the tangential strains in the steel tube were too small in the analyses, when compared with the measured ones. With the second version of the model, larger strains were obtained for the analyses. The reason for this can be seen directly in Figure 17, where the second expression for the upper limit gives greater splitting stress than the first one for the same bond stress. This is so when the coefficient of friction is between zero and one, as it is when the maximum capacity at a pull-out failure is obtained. When the coefficient of friction is larger than one, it is the other way around; i.e. the second expression for the upper limit gives a lower splitting stress than the first one for the same bond stress. Since the largest value of the coefficient of friction was 1.0 in the calibration of the second version, however, this example is not valid here.
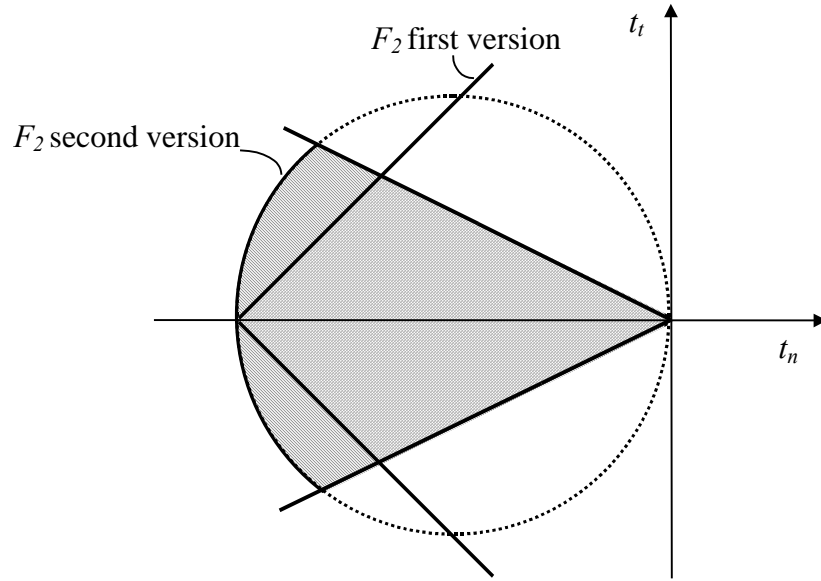
Figure 17   Comparison of the yield lines for the two versions of the model.

4.2.2   Splitting stress in the damaged deformation zone

In the first version of the bond model, it was assumed that the splitting stress decreased during unloading until the bond stress was zero, and then increased again when bond stress in the opposite direction was obtained. The results from the cyclically loaded steel-encased pull-out tests showed, however, that this was not so. As can be seen in Figure 18, the tangential strain in the steel tube decreased during unloading, on the other hand, it continued to decrease also when there was a small bond capacity in the opposite direction. The tangential steel strain did not start to increase again until the reinforcement had returned to its original position, most clearly shown in Figure 18 (b). This means that the splitting stresses due to the bond action do not start to increase again until the slip is back to zero. The relation between the tractions **t** and the relative displacement **u** in the elastic range was accordingly changed from equation (1) in Paper I to (1) in Paper III:

$$\begin{bmatrix} t_n \\ t_t \end{bmatrix} = \begin{bmatrix} D_{11} & \dfrac{t_t}{|t_t|}D_{12} \\ 0 & D_{22} \end{bmatrix} \begin{bmatrix} u_n \\ u_t \end{bmatrix} \tag{6}$$

was changed to

$$\begin{bmatrix} t_n \\ t_t \end{bmatrix} = \begin{bmatrix} D_{11} & \dfrac{u_t}{|u_t|} D_{12} \\ 0 & D_{22} \end{bmatrix} \begin{bmatrix} u_n \\ u_t \end{bmatrix} . \tag{7}$$

Also, the plastic potential function G was changed slightly, from

$$G = |t_t| + \eta(t_n - t_{n0}) = 0 \tag{8}$$

to

$$G = \frac{|u_t|}{u_t} t_t + \eta t_n = 0 . \tag{9}$$

With these changes, the splitting stress and the bond stress decrease until the reinforcement is back in its original position, see Figure 19.
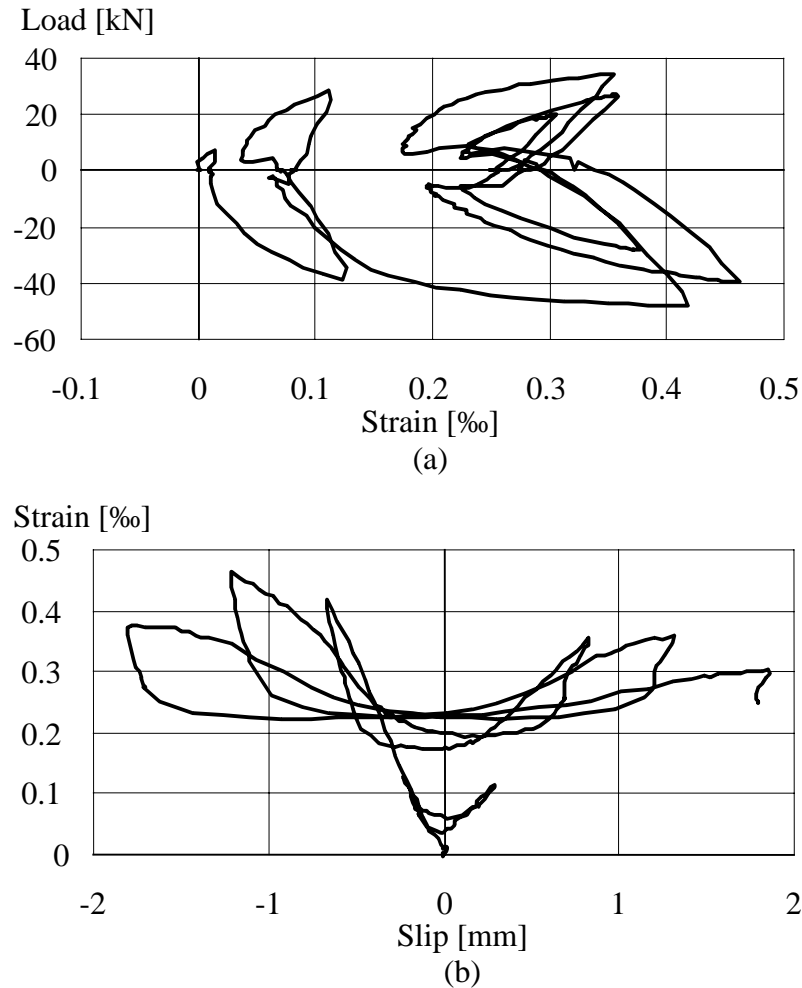
Figure 18   Results from the first load cycles in the steel-encased pull-out test
No. C-0.5b: (a) Load versus tangential strain in the steel tube, and
(b) Tangential strain in the steel tube versus slip.

(a)

(b)
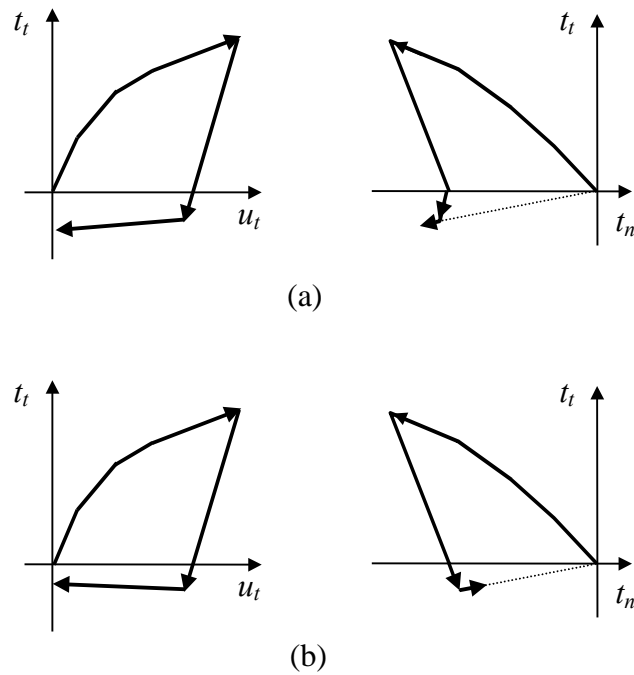
Figure 19 Comparison of results for the two versions of the model, at unloading back to the original position: (a) The first version, and (b) the second version.

4.2.3 The apex of the yield lines

In the first version of the bond model, the apex of the yield lines was moved in the direction of the loading, see Figure 20. The main reason for this was that the increase of the splitting stress within the damaged deformation zone led to an increase of this stress for each successive load cycle. With this large splitting stress, there could also be a large bond stress, when the apex of the yield lines remained at the origin. To avoid this large bond stress, which did not correspond with experimental results, the apex of the yield surface was moved. When, in the second version of the model, the splitting stress decreased until the slip was zero, this stress no longer increased for every load cycle. This seems more reasonable physically. Also, it allows the bond capacity to be reasonably large without moving the apex of the yield lines. The apex therefore remains at the origin in the second version of the model.
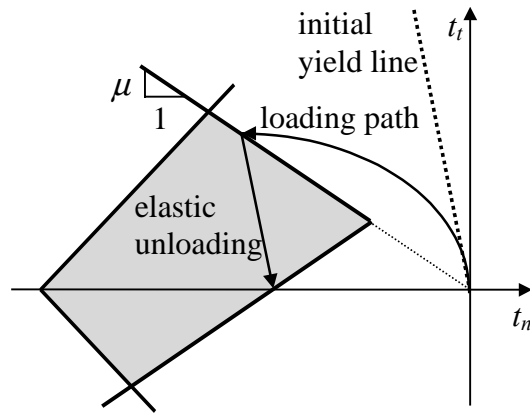
Figure 20   The apex of the yield lines was moved in the direction of the loading in the first version of the model.

4.2.4   The parameters μ and η within the damaged deformation zone

In the first version of the model, the coefficient of friction, μ, and the parameter η were assumed to have constant values within the damaged deformation zone. The parameter η within the damaged deformation zone, η_d, was set so low that the bond stress was almost constant in this zone. When the undamaged deformation zone was reached, a steep increase was obtained, see Figure 21 (a). A cyclic pull-out test by Balázs and Koch (1995) was analysed in which the force was applied on one end of the reinforcement bar, so the slip was not constant along the reinforcement bar. This variation of the slip along the bar made the load increase in the analysis slightly less abrupt than the increase in local bond stress, although this load increase was not as gradual as was observed in their tests, see Figure 7 in Paper I.
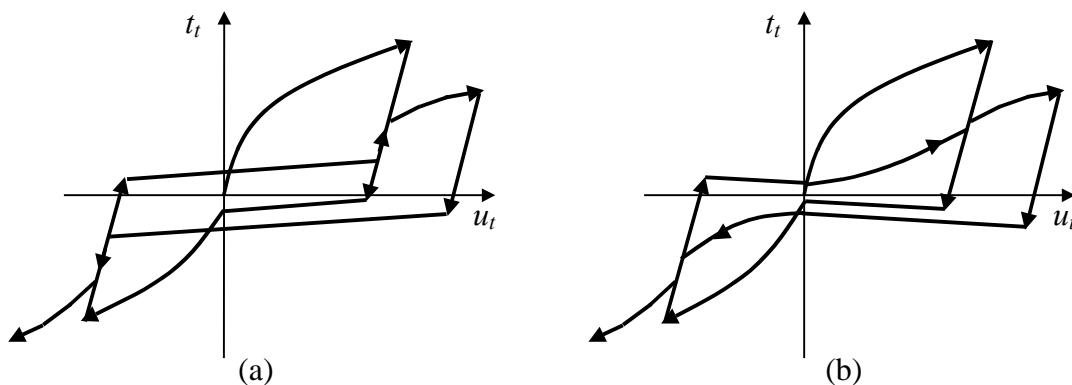
Figure 21   Bond stress versus slip: results from (a) the first version, and (b) the second version of the model.

However, the steel-encased pull-out tests were loaded in a rigid frame, so that both ends of the reinforcement bar were active. The variation of the slip along the bar was thus very close to zero. In the analysis, the abrupt increase of the bond stresses when reaching the undamaged deformation zone therefore gave a corresponding abrupt increase in the load versus slip curve. Since this was not the case for the measured results, a revision of the model was indicated.

In the first version of the model, it was assumed that there were "empty holes" in the concrete in the range of the passed slip. In the second version of the model, the concrete that is crushed in front of the ribs was taken into account. While the crushed concrete can still have some capacity to carry compressive load, it has no capacity at all in tension. Consequently, the friction was assumed to vary in the damaged zone according to whether loading was applied in the direction away from, or towards, the original position. It was assumed to drop immediately to a low value at load reversal, and to keep this value until the original position was reached. For further loading, away from the original position, the friction was assumed to increase gradually, until the undamaged zone was reached, when the normal value was used again. To describe this gradual increase, an equation of the second degree was chosen. In Figure 22, a comparison of the two versions of the model is shown.
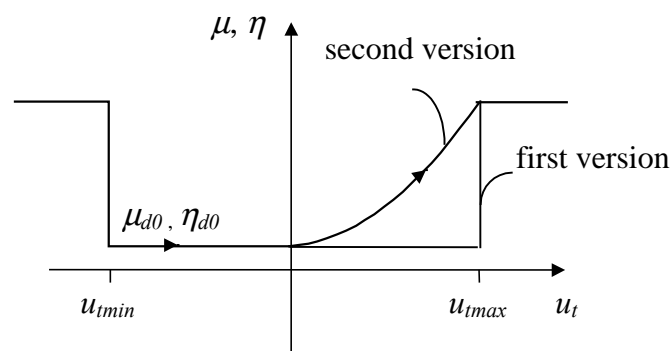
Figure 22   The coefficient of friction, μ, and the parameter η in the damaged deformation zone. Comparison of the two versions of the model.

4.3   Calibration of the Model

The different versions of the model were calibrated against pull-out tests found in the literature; the second version was also calibrated against the steel-encased pull-out tests that are presented in Paper II. In order to investigate whether the model could also describe the loss of bond when the reinforcement was yielding, a degree project was carried out, see Haga and Olausson (1998), in which the first version of the model was used. Since the calibration of the model was not quite finished, the input parameters used were slightly different from the ones described in Paper I. Some changes in the input assumptions were also made for the second version of the model, compare Paper I with Paper III. In Figure 23 it can be seen that the coefficient of friction was set slightly lower in the second calibration, to match the large tangential strains that were measured in the steel-encased pull-out tests. Also the other parameters were subjected to minor changes, for example the parameter η was changed from 0.05 to 0.04.

Another, and perhaps more significant, change between the calibrations of the two versions is that, for the second version, the stiffnesses in the stiffness matrix, **D**, were assumed to be determined by the modulus of elasticity of the concrete rather than by the compressive strength. The reason for this was further consideration about what the stiffnesses physically described, and how they can be derived. The stiffnesses in the elastic stiffness matrix, **D**, shall describe how the concrete between the ribs acts for elastic conditions. In Appendix A it is shown how these stiffnesses were derived.
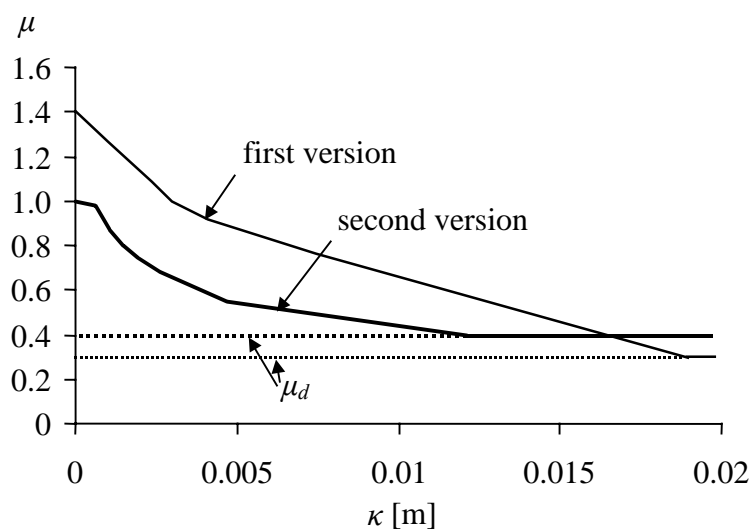
Figure 23   The coefficient of friction versus the hardening parameter: input chosen.

4.4   General Remarks

The new bond model was calibrated for reinforcement bars K500 φ 16 and normal strength concrete (cylinder compressive strength about 30 MPa). However, the calibration was made in such a way that the stiffnesses and the strength were expressed in terms of modulus of elasticity and strength of the concrete. After this calibration, Magnusson (2000) used the model in analyses of tests for which the same type of reinforcement was used, although the concrete was a high strength one with cylinder compressive strength of about 100 MPa. Since the analyses showed good agreement with the tests, it seems as if the calibration is also applicable to concrete of other qualities. The main reason for this is that the parameters are physically meaningful, not chosen arbitrarily. Nevertheless, it must be emphasised that the way the surrounding structure is modelled is critical. If splitting of the concrete dominates the failure mode, parameters such as the fracture energy and the tensile strength of the concrete are crucial.

Concerning other types of reinforcement bars, it is not very likely that the same calibration will give good results. The stiffnesses D_{11} and D_{22} were derived for the geometry of a reinforcement bar K500 φ 16, see Appendix A. However, if the same derivations are made for the geometry of another kind of reinforcement bar, they can probably be used. The input of the coefficient of friction will most likely also change if the reinforcement type is changed. If the type of reinforcement is completely different, new comparisons with tests would need to be done, preferably steel-encased pull-out tests for which the tangential strains can be measured.

The model was calibrated with tests that were selected to show five different types of failure; i.e. pull-out failure, splitting failure, pull-out failure after yielding of the reinforcement, rupture of the reinforcement bar, and cyclic loading. The results show that the model is capable of dealing with all these kinds of failure modes in a physically meaningful way, and reasonably good agreement between analyses and experimental results was found, see Paper III. On the other hand, there are still other parameters that are known to influence the bond action. Two such parameters are the presence of outer pressure, and shrinkage of the concrete; although the model was not specifically calibrated with any tests for these two parameters, the behaviour of the model was observed in relation to their presence or absence.

4.4.1 Outer pressure

Pull-out tests with short embedment length, Magnusson (1997), were analysed without any outer pressure, for Paper III. Here, an outer pressure of 5 MPa was applied, and kept constant while the pull-out force was applied. The results are compared with results from the analysis without outer pressure, see Figure 24. While the outer pressure was applied, the radial deformation between the reinforcement bar and the concrete decreased, which implies a normal stress t_n, see Figure 25. This means that, when slipping between the concrete and the reinforcement began, some normal stresses were already present. Therefore, the first part of the loading was elastic, until the yield line was reached. Thus, the load versus slip starts with a stiff, elastic part. The capacity is, however, not influenced, since the failure mode is pull-out failure in both cases; the pull-out failure in the model is governed by the upper limit in the form of the yield line, F_2, which is determined from the compressive strength of the concrete. Test results of Robins and Standish (1984) indicate that this is a correct behaviour. They carried out cube pull-out tests with deformed bars with lateral pressure varying from 0 to 28 MPa. They concluded that the maximum capacity was increased for low levels of confinement, since the failure mode was changed from splitting failure to pull-out failure. On the other hand, further increase of the lateral confinement had no influence on the maximum capacity.
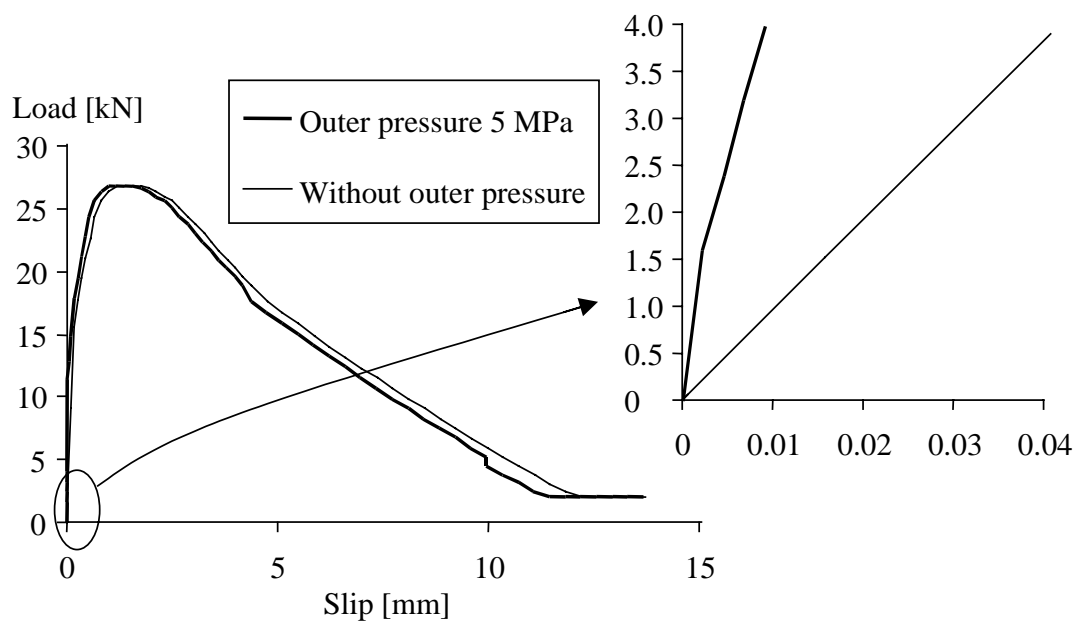
Figure 24 Comparison of results from analyses of a pull-out test where pull-out failure is limiting, with and without an outer pressure.
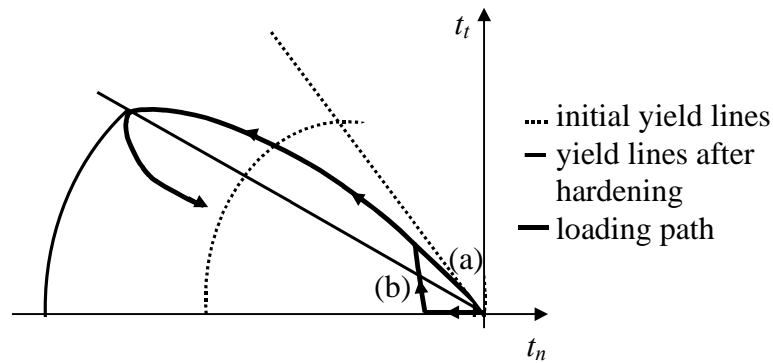
Figure 25   The effect of either outer pressure or shrinkage of the concrete, in the stress space: (a) Without outer pressure and shrinkage of the concrete, and (b) With either an outer pressure or shrinkage of the concrete taken into account.

There are tests described in the literature that report a higher capacity due to outer pressure. However, when these references were read more thoroughly, it appeared that splitting cracks were present, Untrauer and Henry (1965), Eligehausen *et al.* (1983). As these splitting cracks had probably reduced the capacity, the presence of an outer pressure would have a beneficial effect. This also reflects the behaviour of the model presented. The bar pull-out splitting test without spiral reinforcement carried out by Noghabai (1995), see Paper I, was analysed both with and without a confining outer pressure. In the analysis without outer pressure, failure was due to splitting of the concrete. As can be seen in Figure 26, an outer pressure then increased the capacity. In this example, the applied outer pressure was great enough to prevent the development of splitting cracks; thus, the capacity was increased to the level of a pull-out failure. For a low confining pressure, the formation of the splitting cracks would only have been delayed, meaning that the capacity would have been greater than for the unconfined specimen, although not enough to lead to a pull-out failure.
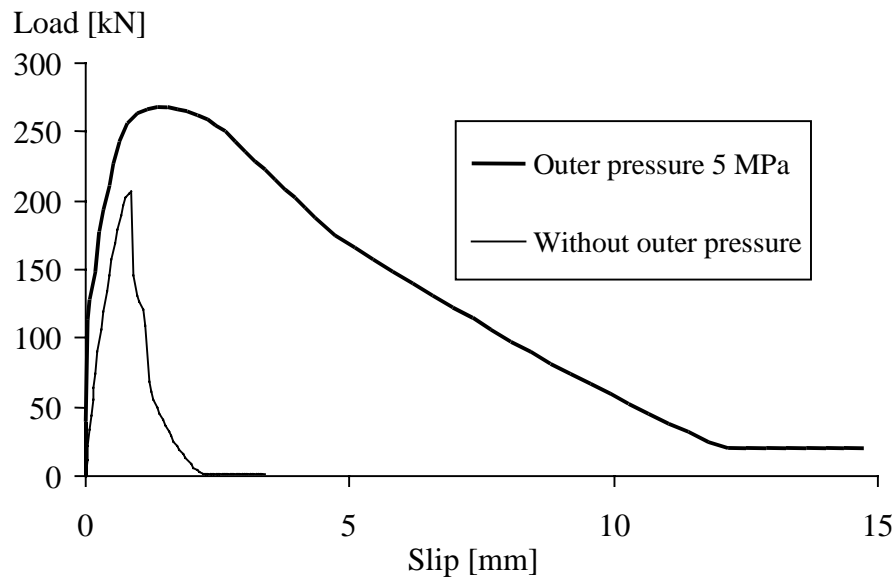
Figure 26 Comparison of results from analyses of a pull-out test where splitting failure is limiting, with and without an outer pressure.

Magnusson (2000) has applied the model in some analyses of beam ends. The beam ends were either supported at their lower edge, so that the support reaction gave confinement to the reinforcement anchored over the support, or they were hung, so that the support reaction acted over the reinforcement bars, i.e. there was no confinement. It appeared from the analyses that the model could describe the behaviour accurately, and reasonably good agreement was found between the analyses and the test results. When no confinement was present, splitting failure occurred, which reduced the anchorage capacity in both the analyses and the tests. The confinement made it possible to obtain a pull-out failure in the analyses, i.e. the capacity was increased by about as much as in the tests. From these tests and analyses, it seems as if the model can also describe the effect of outer pressure in a reasonable way. The results indicate that outer pressure can increase the bond capacity to the limit of the pull-out failure, although no further.

4.4.2 Shrinkage

The adhesion between the concrete and the reinforcement bar is assumed to be negligible in the new bond model. On the other hand, in pull-out tests it is usual to have a first part of the load versus slip curve that is very stiff; this part is usually said to be due to the adhesion. However, a part of it may be caused by shrinkage of the concrete. When the concrete around the reinforcement bar shrinks, there are normal stresses between the concrete and the reinforcement bar before slipping starts. This resembles the situation with outer pressure discussed before, see Figure 25. Yet there is a difference which is that the shrinkage of the concrete also causes tensile stresses around the reinforcement bar, so that splitting cracks could appear. This is in contrast to the application of outer pressure which does not give rise to any tensile stresses.

The pull-out tests with short embedment length, Magnusson (1997), were analysed both with and without shrinkage of the concrete being taken into account. A shrinkage strain of $-1.1 \cdot 10^{-5}$ was then applied, calculated from CEB (1993), taking into account how the test specimens were stored. The results are compared in Figure 27. As can be seen, the first part is stiffer when shrinkage is taken into account. However, for larger values of the slip, there is no difference between the two analyses.
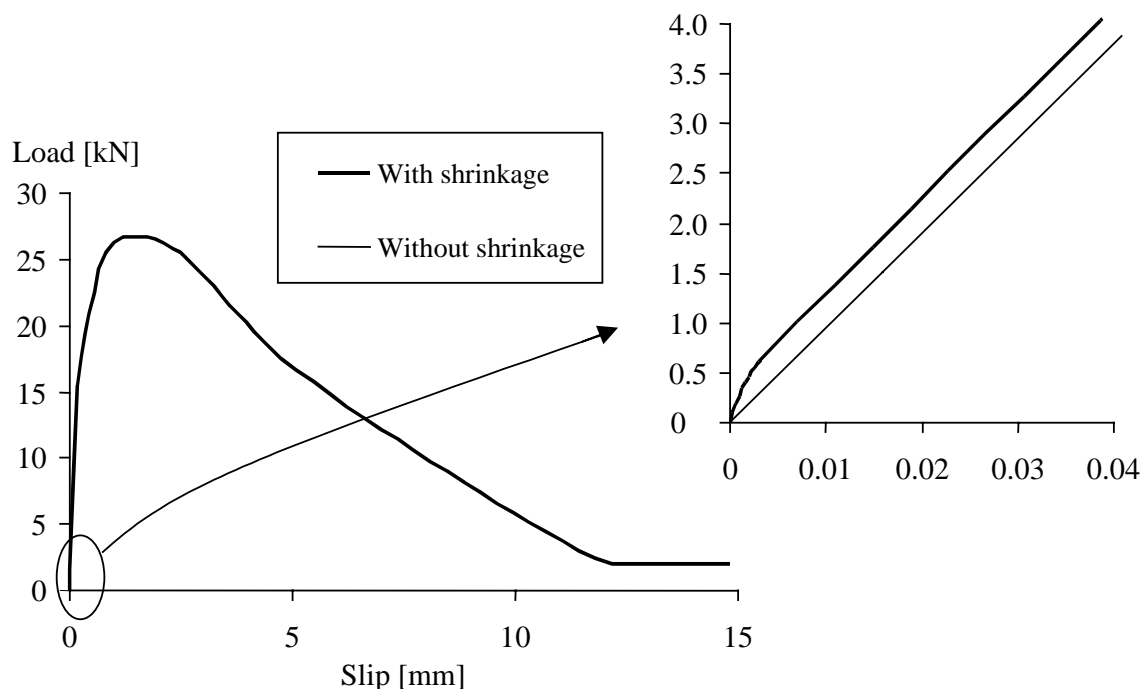
Figure 27   The results from analysis of a pull-out test, with and without shrinkage of the concrete taken into account.

34

5 FRAME CORNERS SUBJECTED TO CLOSING MOMENTS

Frame corners have been investigated by several researchers. Experimental work, for example Mayfield *et al.* (1971) and Nilsson (1973), has shown that frame corners subjected to opening moments are more sensitive to the method of detailing in the reinforcement than those subjected to closing moments. Hence, most publications for the past few decades have concentrated on opening moments. In the Swedish Standards, Boverket (1994), it is recommended *not* to splice the reinforcement within a corner region and, until recently, this has not been allowed by the Swedish Road Administration, see Vägverket (1994). The reason for this was that for opening moments the behaviour of the corner is sensitive to the detailing of the reinforcement. Although corners subjected to closing moments were less well investigated, splices were not allowed for this type either. The aim of this work was to investigate whether splicing of the reinforcement can be allowed, at least for closing moments. In this section, the structural behaviour of frame corners subjected to closing moments is discussed. For a literature survey of work carried out on frame corners, see Nilsson (1973) which treats work done before 1973 and Karlsson (1999) for later work, or Johansson (2000).

5.1 Internal Forces in a Corner Subjected to Closing Moment

The internal forces in a corner subjected to a closing moment are shown in Figure 28. After cracking of the concrete, the tensile forces are carried by the reinforcement, as shown in Figure 28 (b). If the corner is well-designed, failure will be due to bending in the sections adjacent to the corner, with yielding of the reinforcement. According to Stroband and Kolpa (1983), there are three possible failure modes that will cause premature failure of the corner.

<div style="text-align:center">(a)   (b)</div>
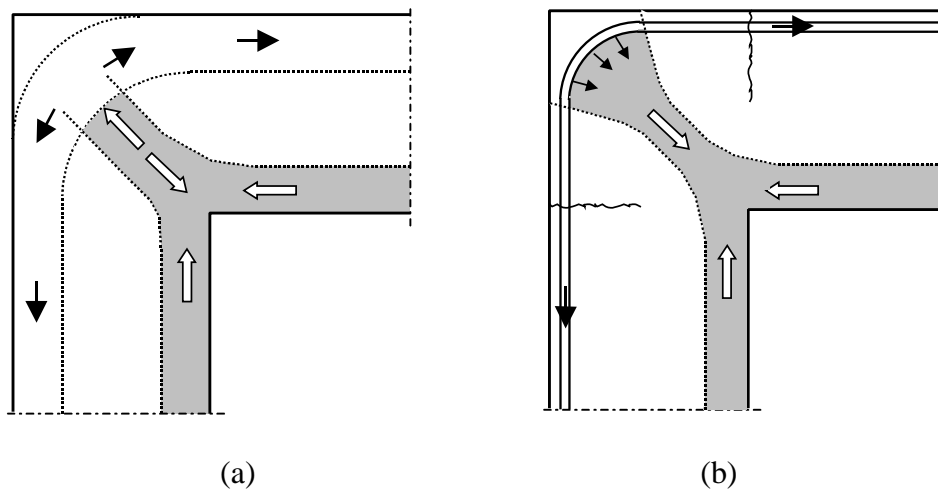
Figure 28   The internal forces in a corner subjected to a closing moment: (a) Uncracked corner, and (b) corner with bending cracks. From Stroband and Kolpa (1983).

- Crushing of the concrete in the compressive zone

  For elastic materials, there are stress concentrations at corners. For a corner subjected to closing moment, this leads to large compressive stress at the inner part of the corner. However, when the concrete reaches the plastic stage, this stress concentration is no longer so pronounced. Furthermore, there will be a biaxial compressive state, due to the compressive stresses from both sides of the corner, or even a triaxial stress state if lateral deformations are restricted. Thanks to this bi- or triaxial compressive stress state, the concrete will have a greater capacity, and also more ductility. However, as shown in Paper IV, the tested corner specimens were very close to this failure mode.

- Crushing of the concrete in the compressive diagonal

  In Figure 28, where the internal forces in a corner subjected to a closing moment are shown, it can be seen that the compressive zones from each part of the corner are balanced by a compressive diagonal. If the stress in this compressive diagonal becomes large, crushing of the concrete might occur.

- Bearing failure at the bend of the reinforcement

  When a reinforcement bar is bent, radial compressive stresses are present, see Figure 29 (a). When these compressive stresses spread, as shown in Figure 29 (b), tensile stresses act out of the plane of the bar curvature. If these tensile stresses

become too large, splitting cracks will appear. At first, this type of failure was thought to be important in combination with reinforcement splices. Splicing the reinforcement also causes splitting stresses, and it was believed that the combination of these effects could cause splitting cracks that would reduce the bond capacity. Nevertheless, the tests and analyses presented in Paper IV show that this did not happen. Note, however, that bearing failure at the bend of the reinforcement is more likely to occur near a reinforcement bar close to a free edge. The main interest of this study is corners in bridges. Here, the corners have a long extension with a large number of reinforcement bars. Furthermore, the edges are usually not free; they are connected to other parts of the structure. Accordingly, the failure mode with a splitting side cover is of no special interest in this study. For the corners of beams, in particular when only two reinforcement bars are present, the effect of the edges is of course much greater. Splitting of the side cover must then be prevented, in order to avoid premature failure of the corner.

For these types of failure, the strength of the concrete is critical. In the first and second failure types discussed, premature crushing of the concrete, it is the compressive strength that is decisive. Also the amount of reinforcement is important: the larger the amount of reinforcement, the greater the forces the concrete must be able to carry. Stroband and Kolpa (1983) derived an analytical expression for how much reinforcement can be allowed; this was to avoid the premature failure of the concrete in the compressive diagonal. In the third type of failure, bearing failure at the bend of the reinforcement, it is mainly the tensile strength that has an influence on the result, and also the thickness of the concrete cover.

(a)   (b)
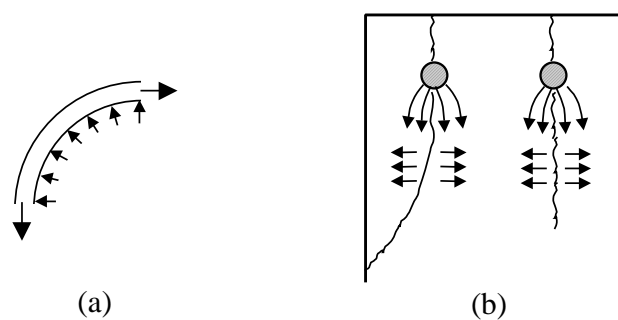
Figure 29   Bent reinforcement bar causing (a) radial compressive stresses and (b) splitting stresses out of the plane of the bar curvature.

For a spliced corner, there is also a fourth type of premature failure:

- Anchorage of the reinforcement

  If the anchorage of the reinforcement is not adequate, premature failure of the corner will occur. To avoid this, a minimum splice length is required. The tests and analyses presented in Paper IV show that the splice lengths required by the existing codes are sufficient.

Altogether, this shows that splicing the reinforcement within a corner region does not seem to have any negative effect on the behaviour of the corner, since the behaviour of the spliced corner differs only a little from a corresponding unspliced corner. The same conclusion has been drawn in Stroband and Kolpa (1983), Plos (1994a, 1994b, 1995), Johansson (1995, 1996a, 1996b), Lundgren and Plos (1996), and Olsson (1996). However, it is worth noting that, for certain conditions, the capacity of a corner (spliced or unspliced) is less than the capacity of the adjoining sections. For corner regions with free edges, splitting of the side cover must be prevented, either with a sufficient thickness of the concrete cover or with confining reinforcement. When this is done, or if the corner region does not have free edges, the capacity of the corner is greater than the capacity of the adjoining sections for the concrete qualities and amount of reinforcement that are usually used today. For the low concrete qualities that were used some years ago (with a compressive strength as low as about 15 MPa), premature failure of the corner might occur. Also, if the capacity of the steel were dramatically increased beyond what is normal today, or very large amounts of reinforcement were used, premature failure of the corner might occur.

5.2 Frame Corners Subjected to Cyclic Loading

Frame corners subjected to closing moments and cyclic loading have been investigated by Plos (1994b, 1995). In that investigation, spliced and unspliced specimens were compared. Even though all of the reinforcement was spliced in the same cross-section, no disadvantage in splicing the reinforcement could be found. All of the tests resulted in fatigue of the reinforcement.

The results from the static analyses and tests indicate that reinforcement splices in a corner region behave in about the same way as reinforcement splices in beams.

Probably, the same is valid also for cyclic loading. Therefore, there is little reason to believe that it would be more dangerous to splice the reinforcement within the corner region than outside it. The behaviour of lap splices in beams subjected to cyclic loading has been examined by many researchers. A summary of the results can be found in ACI (1992). By following the design rules for splices subjected to cyclic loading, a sufficient level of safety can be obtained.

5.3   Tests and Analyses of Frame Corners

Tests and analyses within an earlier part of the project, "Detailing of frame corners in concrete bridges", did not reveal any disadvantages in splicing the reinforcement within a frame corner. Hence, it was decided to investigate the worst case. Here, a brief summary of the study is given; for more details see Paper IV or Lundgren (1999b). Four frame corners with differing detailing were subjected to a closing moment, combined with shear and a normal force. The detailing of the main reinforcement is shown in Figure 30. One corner had unspliced reinforcement, (a), while another had spliced reinforcement with the splice length required by the codes, (b). The two last frame corners, (c) and (d), had spliced reinforcement with a splice length that was less than half of that required by the codes. All of the test specimens had a relatively high amount of reinforcement; the main reinforcement was placed in one layer, and the distance between the main reinforcement bars was the minimum distance allowed according to the Swedish Standards, Boverket (1994). The reason for these choices was to investigate what was considered to be the worst case.
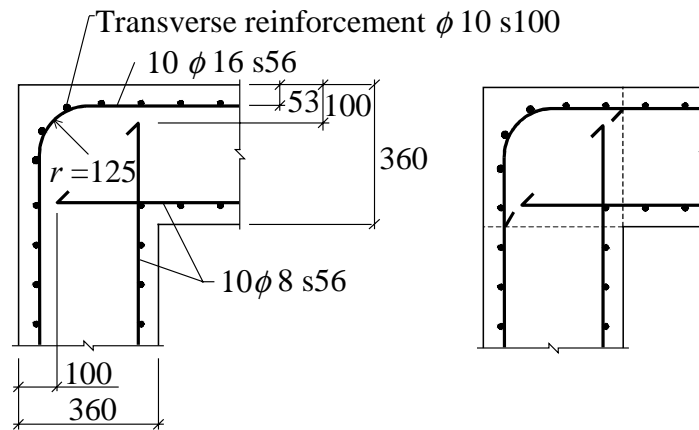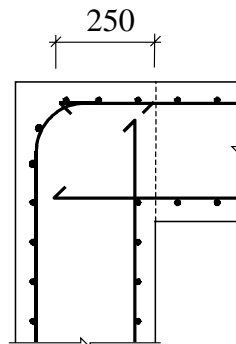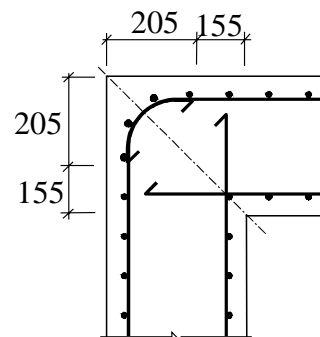
Figure 30 Detailing of the reinforcement in the corners of the test specimens. Measurements, compressive and transverse reinforcement in (b), (c) and (d) were the same as in (a). Dimensions given in mm.

The tests with unspliced reinforcement and with a long splice showed very similar behaviour, with the maximum capacity determined by the bending capacity of the adjoining cross-sections. After yielding of the reinforcement, concrete began to spall off at the inner part of the corner, in the compressive zone. Thereafter, inclined cracks in the concrete led to a sudden failure in the test with unspliced reinforcement; the test with the long splice was interrupted before this stage.

In one of the tests with a short splice length, centred in the corner, only slightly less capacity than in the unspliced test was obtained. The failure here was caused by the rather sudden appearance of an inclined crack in the concrete, after yielding of the reinforcement. In the other test with a short splice length, with the splice placed

outside the bend of the reinforcement, fracture of the splice limited the capacity, which was then only about half of the capacity of the unspliced corner.

Furthermore, detailed three-dimensional non-linear finite element analyses of the corner regions of the frame corners tested were carried out. The second version of the developed model was used to describe the bond mechanism; thus, the splitting stresses resulting from the anchorage were taken into account. The results from these analyses show that the overall behaviour of the specimens could be quite well described; in all of the analyses the failure mode was the same as in the tests. In particular, it was noted that the fracture of the splice in the specimen with the splice situated outside the bend of the reinforcement was described realistically in the analyses.

Frame corners in large portal bridges have considerably larger dimensions than the specimens tested. Therefore, a large frame corner was also analysed. It had dimensions large enough for one splice, with a splice length as required in the codes, along one of the sides of the corner. The analysis showed that the maximum capacity was determined by the bending capacity of the adjoining cross-sections; i.e. the capacity of the splice was enough so that it was not limiting.

In conclusion, the tests and analyses show that splicing the reinforcement in the middle of the corner has advantages over splices placed outside the bend of the reinforcement. They also indicate, in agreement with the previous analyses and tests, that provided the splice length is as long as required in the codes, there are no disadvantages in splicing the reinforcement within the corner of a frame.

6 CONCLUSIONS AND SUGGESTIONS FOR FUTURE RESEARCH

From the work that has been carried out, the following conclusions can be drawn. The first version of the proposed bond model could describe the behaviour of the bond mechanism relatively well. The results from the steel-encased pull-out tests, however, provided new information about the bond mechanism, in particular for cyclic loading. Consequently, some drawbacks to the first version of the model became apparent. This method of combining theoretical modelling with experimental work is believed to give better results and, perhaps most valuable, to give a deeper understanding of the problem studied than if the work were limited to only one of these aspects. The bond model could thereby be further developed, and the second version of the model is believed to reflect reality quite closely. Analyses of pull-out tests with differing geometries and with both monotonic and cyclic loading showed that the new model is capable of dealing with a variety of failure modes, such as pull-out failure, splitting failure, and the loss of bond when the reinforcement is yielding, as well as dealing with cyclic loading in a physically reasonable way. Results from Magnusson (2000) also indicate that the effect of outer pressure is well described by the improved version of the model.

The refined model was used in detailed three-dimensional analyses of frame corners, to investigate the effect of splices within the corner region. When compared with results from tests on the frame corners, it was found that the analyses could describe the test results in a reasonable way. In particular, it was noted that the fracture of the splice was described closely in the analyses. The tests and analyses showed that splicing the reinforcement in the middle of the corner has advantages over splicing placed outside the bend of the reinforcement. They also indicate, in agreement with previous analyses and tests, Plos (1995), that provided the splice length is as long as required by the codes, there are no disadvantages in splicing the reinforcement within the corner of a frame subjected to closing moments.

The proposed bond model can also be used in other analyses where the bond mechanism plays an important role. It is believed to be a powerful tool for parameter studies of, for example, the effect of transverse reinforcement, anchorage at end

42

supports under different conditions, and rotation capacity. Such parameter studies can serve as a basis for design codes. The model is calibrated for normal strength concrete, but analyses by Magnusson (2000) show that this calibration also gives satisfactory results for high strength concrete. Hence, it is likely that the calibration would also be useful for other types of concrete, e. g. light weight concrete or fibre reinforced concrete. Nevertheless, for each new application, it is recommended that analyses be compared with experimental data first. This is recommended especially if the model is intended to be used for other types of reinforcement bars. Since changing the geometry of the ribs would most definitely affect the friction between the concrete and the reinforcement bar, the calibration of the model would need to be revised for this.

The finite element analyses were all carried out using the finite element program DIANA. These analyses show clearly the advantage of using a rotating crack model instead of fixed crack directions. In some of the analyses, both types of material models gave the same result, while in the analyses where the direction of the principal stress was changed after cracking had occurred, the rotating crack model gave results that corresponded more closely to the measured response. Even though DIANA is believed to have the best material models for concrete among commercial programs today, the material models used to describe concrete still need to be improved. For example, when the material model used is subjected to triaxial compressive stress states, it does give an increase in capacity that seems to correspond well with the measured one, but the increase in ductility appears to be too low for some stress states. Another problem is how to take into account the effect of localisation in compression. Although some research exists in this field, still more needs to be done, especially when combining localisation with triaxial stress states. Furthermore, it ought to be possible to take cyclic loading into account in a more generalised way. At present, the only material models available that can deal with cyclic loading are one-dimensional. The establishment of three-dimensional material models that can cope with cyclic loading would be most useful.

REFERENCES

This list of references also includes those in Papers I to IV.

ACI (1992): *State-of-the-Art Report on Bond Under Cyclic Loads*. Reported by ACI Committee 408. ACI 408.2R-92, ACI, Michigan, 1992.

Al-Fayadh, S. (1997): *Cracking Behaviour of Reinforced Concrete Tensile Members*. Chalmers University of Technology, Division of Concrete Structures, Master's Thesis 97:3, Göteborg, 1997.

Balázs, G. and Koch, R. (1995): Bond Characteristics under Reversed Cyclic Loading. *Otto Graf Journal*, Vol. 6 1995, pp. 47—62.

Balázs, G. (1991): Fatigue of Bond. *ACI Materials Journal*, Vol. 88, No. 6, Nov.-Dec. 1991, pp. 620—629.

Bažant, Z. P. and Oh, B. H. (1983): Crack band theory for fracture of concrete. *Materials and Structures*, RILEM, Vol. 16, No. 93, 1983, pp. 155—177.

Bigaj, A. J. (1999): *Structural Dependence of Rotation Capacity of Plastic Hinges in RC Beams and Slabs*. Ph.D. Thesis, Delft University Press, the Netherlands, 1999.

Boverket (1994): *Boverkets handbok om betongkonstruktioner BBK 94, Band 1 – Konstruktion* (Boverket's Handbook for Concrete Structures BBK94, Vol. 1: Design. In Swedish), Boverket, Byggavdelningen, Karlskrona, Sweden, 185 pp.

CEB (1993): *CEB-FIP Model Code 1990*. CEB Bulletin d'Information No. 213/214, Lausanne, 1993.

CEB (1982): *Bond Action and Bond Behaviour of Reinforcement. State-of-the-Art Report*. CEB Bulletin d'Information No. 151, December 1981.

Chen, W. F. and Han, D. J. (1987): *Plasticity for Structural Engineers*. Springer-Verlag, New York, November 1987.

Chen, W. F. (1982): *Plasticity in Reinforced Concrete*. McGraw-Hill, New York, 1982.

Cox, J. V. (1994): *Development of a Plasticity Bond Model for Reinforced Concrete – Theory and Validation for Monotonic Applications*. Naval Facilities Engineering Service Centre, Port Hueneme, USA, 1994.

Eligehausen, R., Popov, E. P., and Bertero, V. V. (1982): Local Bond Stress-Slip Relationships of Deformed Bars under Generalized Excitations. V.4, *Proceedings of the Seventh European Conference on Earthquake Engineering*, Athens, Sept. 1982, pp. 69—80.

Eligehausen, R., Popov, E. P., and Bertero, V. V. (1983): *Local Bond Stress-Slip Relationships of Deformed Bars under Generalized Excitations*. Earthquake Engineering Research Centre, University of California, Berkeley, California, USA, Report No. UCB/EERC 83/23, October 1983.

Engström, B. (1992): *Ductility of Tie Connections in Precast Structures*. Chalmers University of Technology, Division of Concrete Structures, Publication 92:1, Göteborg, 1992.

Goto, Y. (1971): Cracks Formed in Concrete around Deformed Tension Bars. *Journal of ACI*, Vol. 68, April 1971, pp. 244—251.

Gylltoft, K. (1983): *Fracture Mechanics Models for Fatigue in Concrete Structures*. Division of Structural Engineering, Luleå University of Technology, Doctoral Thesis 1983:25D, Luleå, 1983.

Haga, C. K. and Olausson, K. (1998): *Olinjär finit elementanalys av utdragsförsök* (Non-linear finite element analyses of pull-out tests. In Swedish). Chalmers University of Technology, Division of Concrete Structures, Masters Thesis 98:7, Göteborg, 1998.

Hillerborg, A., Modéer, M., and Peterson, P.-E. (1976): Analysis of Crack Formation and Growth in Concrete by Means of Fracture Mechanics and Finite Elements. *Cement and Concrete Research*, Vol. 6, November 1976, pp. 773—782.

Imran, I. and Pantazopoulou, S. J. (1996): Experimental Study of Plain Concrete under Triaxial Stress. *ACI Materials Journal*, V. 93, No. 6, Nov.-Dec.1996, pp. 589—601.

Jirásek, M. (1999): *Numerical Modeling of Deformation and Failure of Materials*. Lecture Notes, Short course taught by Milan Jirásek, Rheinisch-Westfälische Technische Hochschule, Aachen, 3—7 May, 1999.

Johansson, M. (2000): Ph.D. Thesis. Division of Concrete Structures, Chalmers University of Technology, to be published in 2000.

Johansson, M. (1996a): *New Reinforcement Detailing in Concrete Frame Corners of Civil Defense Shelters: Non-linear Finite Element Analyses and Experiments.* Licentiate Thesis. Division of Concrete Structures, Chalmers University of Technology, Publication 96:1, Göteborg, 1996.

Johansson, M. (1996b): *Non-linear Finite Element Analyses of Frame Corners in Civil Defense Shelters.* Division of Concrete Structures, Chalmers University of Technology, Report 96:3, Göteborg, 1996.

Johansson, M. (1995): *New Reinforcement Detailing in Frame Corners in Civil Defense Shelters: Experiments and Fracture Mechanics Analyses.* Division of Concrete Structures, Chalmers University of Technology, Report 95:2, Göteborg, 1995.

Karlsson, M (1999): *Armeringsutformning i ramhörn och knutar* (Reinforcement Detailing in Frame Corners and Joints. In Swedish). Teknikområde Anläggning, NCC Teknik, Göteborg, October, 1999.

Kupfer, H.B. and Gerstle, K.H. (1973): Behaviour of Concrete Under Biaxial Stresses. *Journal of the Engineering Mechanics Division*, ASCE, Vol. 99 1973, pp. 853—866.

Lundgren, K. (1999a): *Modelling of Bond: Theoretical Model and Analyses.* Chalmers University of Technology, Division of Concrete Structures, Report 99:5, Göteborg, 1999.

Lundgren, K. (1999b): *Static Tests of Frame Corners Subjected to Closing Moments.* Chalmers University of Technology, Division of Concrete Structures, Report 99:2, Göteborg, 1999.

Lundgren, K. (1998): *Steel-Encased Pull-Out Tests Subjected to Reversed Cyclic Loading.* Chalmers University of Technology, Division of Concrete Structures, Report 98:9, Göteborg, 1998.

Lundgren, K. and Gylltoft, K. (1997): Three-Dimensional Modelling of Bond. In: *Advanced Design of Concrete Structures* (eds. K. Gylltoft, B. Engström, L.-O. Nilsson, N.-E. Wiberg, and P. Åhman), CIMNE. Barcelona, 1997, pp. 65 - 72.

Lundgren, K. and Plos, M. (1996): *Splicing of Reinforcement in Frame Corners: Finite Element Analyses*. Division of Concrete Structures, Chalmers University of Technology, Report 96:2, Göteborg, 1996.

Magnusson, J. (2000): *Bond and Anchorage of Ribbed Bars in High-Strength Concrete*. Ph.D. Thesis. Division of Concrete Structures, Chalmers University of Technology, to be published in 2000.

Magnusson, J. (1997): *Bond and Anchorage of Deformed Bars in High-Strength Concrete*. Licentiate Thesis. Division of Concrete Structures, Chalmers University of Technology, Publication 97:1, Göteborg, 1997.

Mainz, J. (1993): *Modellierung des Verbundtrag-verhaltens von Betonrippenstahl*. Berichte aus dem Konstruktiven Ingenieurbau, Technische Universität München, 3/93, 1993.

Malvar, L. J. (1992): Confinement Stress Dependent Bond Behavior, Part I: Experimental Investigation. In: *Bond in Concrete Proceedings* (CEB), Riga, 1992, pp.1–79 - 1–88.

Markeset, G. (1993): *Failure of concrete under compressive strain gradients*, Ph.D. Thesis 1993:110, The Norwegian Institute of Technology, Trondheim, 1993.

Mayfield, B., Kong, F.-K. and Bennisson, A. (1971): Corner Joint Details in Structural Lightweight Concrete. *ACI Journal*, May 1971, pp. 366—372.

Nilsson, I. (1973): *Reinforced concrete corners and joints subjected to bending moment*. National Swedish Institute for Building Research, Document D7:1973, Stockholm, 1973.

Noghabai, K. (1995): *Splitting of Concrete in the Anchoring Zone of Deformed Bars: A Fracture Mechanics Approach to Bond*. Licentiate Thesis. Division of Structural Engineering, Luleå University of Technology, 1995:26L, Luleå, 1995.

Olsson, M. (1996): *Olinjär finit elementanalys av ramhörn i armerad betong* (Non-linear Finite Element Analyses of Frame Corners in Reinforced Concrete. In Swedish). Division of Concrete Structures, Chalmers University of Technology, Diploma Work 96:6, Göteborg, 1996.

Plos, M. (1995): *Application of Fracture Mechanics to Concrete Bridges: Finite Element Analyses and Experiments*. Ph.D. Thesis. Division of Concrete Structures, Chalmers University of Technology, Publication 95:3, Göteborg, 1995.

Plos, M. (1994a): *Ny armeringsskarv för ramhörn i skyddsrum* (New reinforcement splice for frame corners in shelters. In Swedish). Division of Concrete Structures, Chalmers University of Technology, Report 94:2, Göteborg, 1994.

Plos, M. (1994b): *Utmattning av ramhörn med skarvad armering* (Fatigue of frame corners with spliced reinforcement. In Swedish). Division of Concrete Structures, Chalmers University of Technology, Report 94:1, Göteborg, 1994.

Reinhardt, H. W., Blaauwendraad, J. and Vos, E. (1984): Prediction of bond between steel and concrete by numerical analysis. *Materials and Structures*, RILEM, Vol. 17, No. 100, 1984, pp. 311—320.

Robins, P. J. and Standish, I. G. (1984): The influence of lateral pressure upon anchorage bond. *Magazine of Concrete Research*, Vol. 36, No. 129, December 1984, pp. 195—202.

Stroband, J. and Kolpa, J. J (1983): *The behaviour of reinforced concrete column-to-beam joints. Part 1. Corner joints subjected to negative moments*. Department of Civil Engineering, Delft University of Technology, Report 5-83-9, Research No. 2.2.7303, Delft, April 1983.

Tassios, T. P. (1979): Properties of Bond between Concrete and Steel under Load Cycles Idealizing Seismic Actions. *AICAP-CEB Symposium, Vol. 1 – State of the Art Reports* (CEB Bulletin d'Information No. 131), Rome, Italy, 1979. pp. 67-122.

Tepfers, R. and Olsson, P.-Å. (1992): Ring Test for Evaluation of Bond Properties of Reinforcing Bars. In: *Bond in Concrete Proceedings* (CEB), Riga, 1992, pp. 1-89 - 1-99.

Tepfers, R. (1973): *A Theory of Bond Applied to Overlapped Tensile Reinforcement Splices for Deformed Bars*. Division of Concrete Structures, Chalmers University of Technology, Publication 73:2, Göteborg, 1973.

Thorenfeldt, E., Tomaszewicz, A. and Jensen, J. J. (1987): Mechanical Properties of High-Strength Concrete and Application in Design. In Proceedings: *Utilization of High Strength Concrete*, Symposium in Stavanger, Norway, 1987. (Tapir N-7034 Trondheim).

TNO Building and Construction Research (1998): *DIANA Finite Element Analysis, User's Manual release 7*. Hague, 1998.

Tomaszewicz, A. (1985): Hoyfast betong arbetsdiagram (2). (High Strength Concrete; Stress versus Strain Diagram. In Norwegian). From *FCBs Informasjonsdag*, Trondheim, 25 October, 1985, Forskningsinstituttet for Cement og Betong.

den Uijl, J. and Bigaj, A. J. (1996): A Bond Model for Ribbed Bars Based on Concrete Confinement. *Heron*, Vol.41, No.3, 1996.

Untrauer, R.E. and Henry, R. L. (1965): Influence of Normal Pressure on Bond Strength. *Journal of the ACI*, Vol. 62, May 1965, pp. 577—586.

Vandewalle, L. (1992): Theoretical Prediction of the Ultimate Bond Strength between a Reinforcement Bar and Concrete. In: *Bond in Concrete Proceedings* (CEB), Riga, 1992, pp. 1-1 – 1-8.

van Mier, J. G. M. (1984): *Strain Softening of Concrete under Multiaxial Loading Conditions*. Ph.D. Thesis, Eindhoven University of Technology, Eindhoven, the Netherlands 1984.

van Mier, J. G. M., Shah, S. P., Arnaud, M., Balayssac, J. P., Bascoul, A., Choi, S., Dasenbrock, D., Ferrara, G., French, C., Gobbi, M. E., Karihaloo, B. L., König, G., Kotsovos, M. D., Labuz, J., Lange-Kornbak, D., Markeset, G., Pavlovic, M. N., Simsch, G., Thienel, K-C., Turatsinze, A., Ulmer, M., van Geel, H. J. G. M., van Vliet, M. R. A., Zissopolos, D. (1997): Strain softening of concrete in uniaxial compression. *Materials and Structures*, RILEM, Vol. 30, May 1997.

Vägverket (1994): *Bro 94 – Allmän teknisk beskrivning för broar* (Bridge 94 – General Technical Description for Bridges. In Swedish). Swedish Road Administration, Borlänge, 1994.

Åkesson, M. (1993): *Fracture Mechanics Analysis of the Transmission Zone in Prestressed Hollow Core Slabs*. Licentiate Thesis. Division of Concrete Structures, Chalmers University of Technology, Publication 93:5, Göteborg, 1993.

Åkesson, M. (1996): *Implementation and Application of Fracture Mechanics Models for Concrete Structures*. Ph.D. Thesis. Division of Concrete Structures, Chalmers University of Technology, Publication 96:2, Göteborg, 1996.

APPENDIX A

DERIVATION OF THE ELASTIC STIFFNESSES

IN THE ELASTIC STIFFNESS MATRIX

The stiffnesses in the elastic stiffness matrix, **D**, describe how the concrete between the ribs behaves under elastic conditions. The dimensions of the ribs on several reinforcement bars K500 ϕ 16 were measured in Al-Fayadh (1997). Here, the average of the measured values are used, see Fig. A-1.
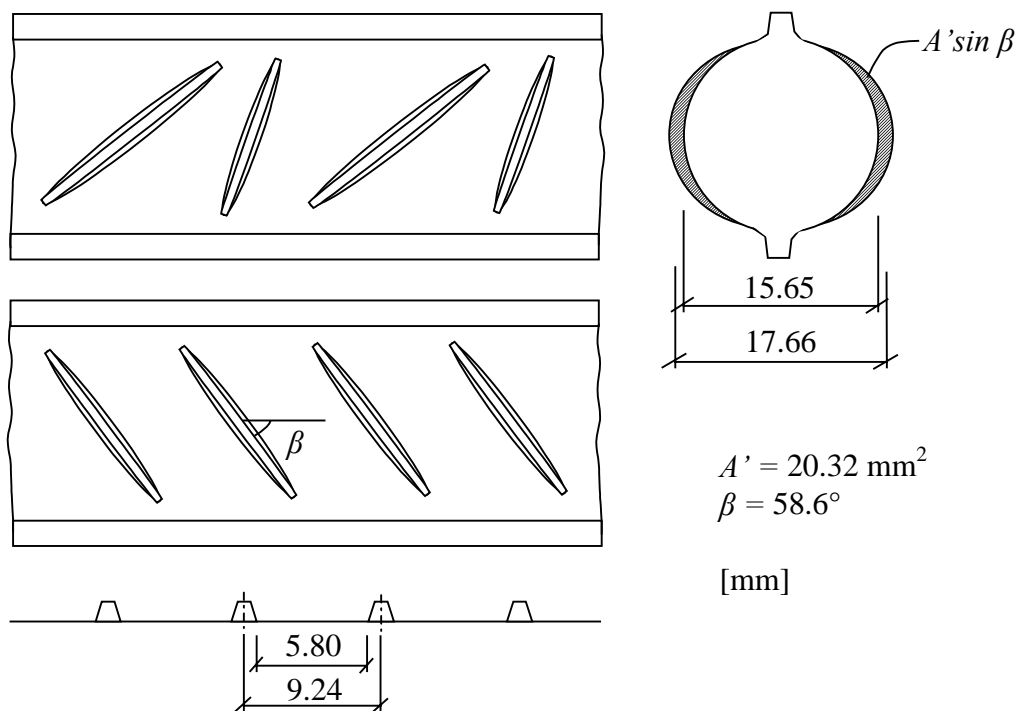
Fig. A-1 Dimensions of the ribs of reinforcement bars K500 ϕ 16. Values are average values from measurements on several bars in Al-Fayadh (1997).

The Stiffness D_{22}

The stiffness D_{22} is the relation between the elastic part of the slip, u_t^e, and the bond stress, t_t. An upper limit of D_{22} can be estimated by assuming that all of the bond stress is carried by one rib, and that the next rib acts as a support, see Fig. A-2.

$$u_t^e = \varepsilon l = \frac{\sigma}{E_c} l = \frac{l}{E_c} \frac{F}{A} = \frac{l}{E_c} \frac{t_t \pi d l_k}{2 A' \sin \beta}$$

$$D_{22} = \frac{t_t}{u_t^e} = E_c \frac{2 A' \sin \beta}{\pi d l_k l} =$$

$$= E_c \frac{2 \cdot 20.32 \cdot 10^{-6} \cdot \sin 58.6°}{\pi \cdot 16 \cdot 10^{-3} \cdot 9.24 \cdot 10^{-3} \cdot \dfrac{\left(9.24 \cdot 10^{-3} + 5.80 \cdot 10^{-3}\right)}{2}} \approx 10 \cdot E_c$$
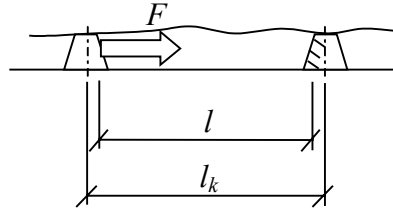
Fig. A-2   Assumptions used to estimate the upper limit of the stiffness D_{22}.

The stiffness D_{22} is also recognised as the stiffness of the first part, or the unloading stiffness, in a bond-slip curve which can be measured experimentally. Since it is difficult to measure the small deformations of the first part, the unloading stiffness was used, see Fig. A-3. Balázs and Koch (1995) measured a value of about $4 \cdot 10^{11}$ N/m^3 for concrete with a wet cube compressive strength of about 30 MPa. This corresponds to about $13 \cdot E_c$. In the cyclically loaded steel-encased pull-out tests, the stiffness was approximately $8 \cdot 10^{10}$ N/m^3 for concrete with a wet cylinder compressive strength of about 35 MPa, which corresponds to about $2.5 \cdot E_c$. The stiffness was chosen to be somewhere between the two measured results, and below the upper limit in the first equation:

$$D_{22} = K_{22} \cdot E_c, \quad K_{22} = 6.0 \, \text{m}^{-1}. \tag{A-1}$$
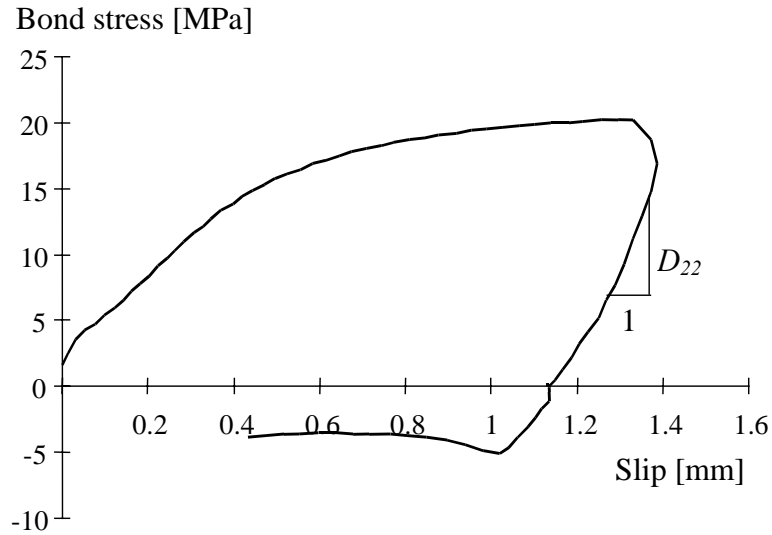
Fig. A-3   The stiffness D_{22} is the unloading stiffness in a bond-slip curve.

The Stiffness D_{11}

The stiffness D_{11} describes the relation between the elastic part of the radial deformation, u_n^e, and the splitting stress, t_n. This stiffness was estimated by examining the concrete between the ribs. The geometry was approximated as a thin ring with an inner radius the same as the smallest radius of the reinforcement bar (without the ribs). The outer radius was determined by the condition that the cross-sectional area of the ring should equal the cross-sectional area of the ribs projecting from the bar core, compare Fig. A-1 and Fig. A-4.

$$r_a = \frac{d_i}{2} = 7.82 \text{ mm, see Fig. A - 1}$$
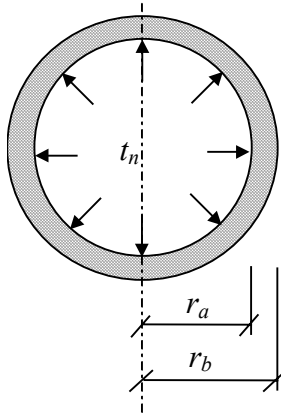
$$2A'\sin\beta = \pi\left(r_b^2 - r_a^2\right)$$

$$r_b = \sqrt{\frac{2A'\sin\beta}{\pi} + r_a^2} =$$

$$= \sqrt{\frac{2 \cdot 20.32 \cdot 10^{-6} \sin 58.6°}{\pi} + \left(7.82 \cdot 10^{-3}\right)^2} =$$

$$= 8.50 \text{ mm}$$

Fig. A-4   Approximated geometry to estimate the stiffness D_{11}.

The outer edges of the ring were assumed to be free, i.e. only the structural behaviour of the ring itself was taken into account. The deformation at the distance r from the centre of a ring is, according to Chen and Han (1987),

$$u_n^e = \frac{(1+\upsilon)\cdot r_a^2 t_n}{E_c\left(r_b^2 - r_a^2\right)} \cdot \left(\frac{(1-2\upsilon)\cdot r}{(1+\upsilon)} + \frac{r_b^2}{r} \right)$$

which gives the stiffness D_{11} as

$$D_{11} = \frac{t_n}{u_n^e} = E_c \cdot \frac{\left(r_b^2 - r_a^2\right)}{(1+\upsilon)\cdot r_a^2} \bigg/ \left(\frac{(1-2\upsilon)\cdot r}{(1+\upsilon)} + \frac{r_b^2}{r} \right) =$$

$$= E_c \cdot \frac{\left(0.00850^2 - 0.00782^2\right)}{(1+0.15)\cdot 0.00782^2} \bigg/ \left(\frac{(1-2\cdot 0.15)\cdot 0.008}{(1+0.15)} + \frac{0.00850^2}{0.008} \right) \approx$$

$$\approx 11 \cdot E_c$$

It was also noted that the larger the D_{11} chosen, the more variation there was of the stresses along the reinforcement bar. This variation arises from differences in the strength of the structure modelled, as for example when stirrups are taken into account. Since the derived value of D_{11} gave a physically reasonable variation, D_{11} was designated

$$D_{11} = K_{11}\cdot E_c, \ K_{11} = 11.0\,\text{m}^{-1}. \tag{A-2}$$

The Stiffness D_{12}

The stiffness D_{12} describes the relation between the elastic part of the slip, u_t^e, and the splitting stress, t_n. Thus, it describes how much splitting stress will be caused by a given slip. Since the calibration of the coefficient of friction derives from experimental results, the model is expected to work in such a way that loading occurs along the yield line. Therefore, the elastic loading ought to cause a larger bond stress than that given by the yield line. From Fig. A-5, it follows that

$$\left| D_{11}du_n + D_{12}du_t \right| \cdot \mu < D_{22}du_t \, .$$

To be sure that this condition is fulfilled, the stiffness D_{12} is chosen so that

$$\left| D_{12} \right| < \frac{D_{22}}{\mu} \, .$$

The value of the stiffness D_{12} determines how large a part of the splitting stress remains after unloading. The larger the value of $|D_{12}|$ chosen, the smaller the splitting stress will be after unloading. By comparison with results from experiments, and taking the previous derived expression into account, the D_{12} chosen was

$$D_{12} = -0.9\frac{D_{22}}{\mu_{max}} \, . \tag{A-3}$$
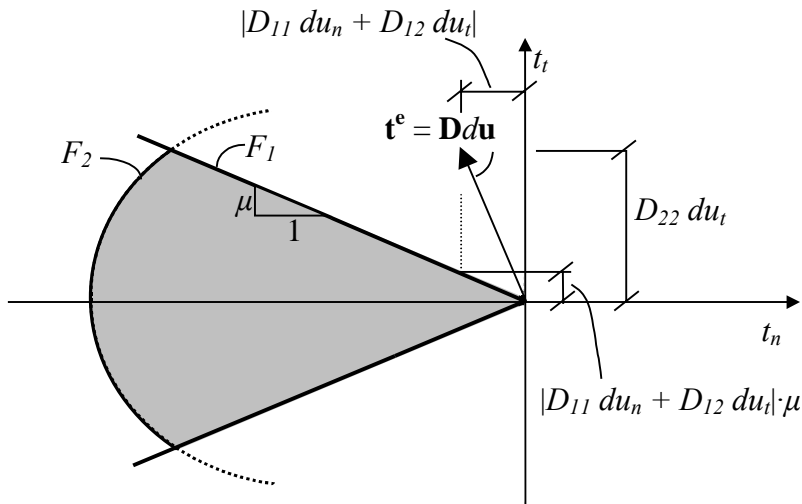
Fig. A-5   The trial stress ought to cause a larger bond stress than is given by the yield line.